Free Kineto-Elastovibration Analysis of High Speed Mechanisms

by

Zongyu Xu

A thesis
Presented to the University of Manitoba
in Partial Fulfillment of the Requirements for the Degree of
Master of Science
in
the Department of Mechanical Engineering

Winnipeg, Manitoba, Canada

April 1990

ISBN 0-315-63262-3

FREE KINETO-ELASTOVIBRATION ANALYSIS OF HIGH SPEED MECHANISMS

BY

ZONGYU XU

A thesis submitted to the Faculty of Graduate Studies of the University of Manitoba in partial fulfillment of the requirements of the degree of

MASTER OF SCIENCE

I hereby declare that I am the sole author of this thesis. I authorize the University of Manitoba to lend this thesis to other institutions or individuals for the purpose of scholarly research.

Zongyu Xu

I further authorize the University of Manitoba to reproduce this thesis by photocopying or by other means, in whole or in part, at the request of other institutions or individuals for the purpose of scholarly research.

Zongyu Xu

Abstract

A systematic approach based on finite element method for the kineto-elasto-vibration analysis of high speed mechanisms is presented. The linearized equations of motion are derived in their most general form via Lagrange's equation. The derivation and the final form of the equations of motion provide the capability to model a general single-loop or multi-loop planar elastic mechanism. Explicit expressions for the resulting mass, damping and stiffness matrices associated with the extra acceleration terms, namely, Coriolis, tangential, normal and pseudo-normal components of elastic accelerations, are listed in Appendix A. The effects of these extra accelerations are clearly identified in the numerical simulations.

Unfortunately, the inclusion of these terms results in non-proportional damping and asymmetric stiffness matrices, producing complex eigensolutions. A general QZ algorithm is employed to solve the complex eigenproblem. Of particular interest in this research is to study and understand how the extra acceleration terms influence the eigenvalues and eigenvectors of high speed flexible mechanisms.

A finite element program has been developed for the investigation. Different simplification analyses are carried out to investigate the effects of the extra acceleration terms on the free kineto-elastovibration characteristics of

high speed mechanisms.

As a numerical example, a four-bar linkage mechanism is analysed, taking account of its rotations. It is found that while Coriolis and tangential acceleration components have negligible influence on the natural frequencies and mode shapes, the effects of normal and pseudo-normal accelerations on the free vibration characteristics of the mechanism are quite significant.

Acknowledgments

The author wishes to express his sincere thanks to Professor Ray P.S. Han for his supervision and financial support throughout the MSc program and during the work on this thesis.

The author would also like to thank his wife for her patience, encouragement and sacrifices.

Contents

List of Figures

List of Tables

Chapter 1

Introduction

1.1 Background

The traditional method employed in mechanism design has been based primarily upon the fundamental assumption that the system is composed of rigid bodies only. No elastic deformations will occur in such a system. This rigid body approach is a reasonably accurate method of design for mechanisms operating at low speeds and has led to the development of a very broad class of mechanisms. However, with the ever increasing demand for high productivity and operating speeds, it is no longer acceptable to assume rigid body motions in mechanisms, especially in situations involving mechanisms constructed of lightweight materials and/or operating at high speeds where the mechanisms may undergo severe elastic deformations due to their own inertia. Therefore, mechanism designers need to develop more advanced mathematical models to predict the response and stability of such elastic systems.

The kineto-elastovibration analysis[1] of high speed mechanisms has been a challenging problem for mechanism designers over the past two decades. The research work involved consists of two aspects, namely free and forced kineto-elastovibration analyses. There has been a tremendous achievement in the latter field with several improvements in theoretical and numerical techniques. Lowen and Chassapis [1], and Thompson and Sung [2] presented two comprehensive reviews of the up-to-date research work in the design and analysis fields of flexible mechanisms. However, there have hardly been published papers regarding free kineto-elastovibration analysis of high speed mechanisms. This thesis attempts to fill this void. Comprehensive studies were paid to the effects of the extra acceleration terms on the natural frequencies and mode shapes of flexible mechanisms in this research. Some fundamental results have been achieved.

In the area of forced kineto-elastovibration analysis of mechanisms, researchers first employed analytical methods to model the problem [3−11]. It soon turns out that such a formulation procedure is always associated with a set of complicated boundary-value problems. To solve more complex problems involving mechanisms with many flexible components, researchers resorted to finite element methods. Both lumped parameter approach and continuum model have been employed.

[1]Computation of vibration characteristics of elastic mechanisms in motion, such as natural frequencies, normal modes, deflections and stresses

Typically by way of finite element method, the linearized equations of motion governing elastic mechanisms with no structural damping may be written as

$$[M]\{\ddot{q}\} + [C]\{\dot{q}\} + [K]\{q\} = \{F\} \tag{1.1}$$

where $[M]$ is the conventional symmetric mass matrix, $[C]$ denotes the motion-induced Coriolis damping matrix[2] due solely to Coriolis acceleration components of elastic deformations, and $[K]$ represents the total stiffness matrix, including the conventional structural stiffness matrix $[K_s]$ and motion-induced stiffness $[K_m]$, i.e.

$$[K] = [K_s] + [K_m] \tag{1.2}$$

It will be shown that $[K_m]$ is composed of the stiffnesses due to tangential, normal and pseudo-normal components of elastic accelerations. These acceleration terms, together with Coriolis acceleration, are defined as extra acceleration terms in this thesis.

Some pioneering work in applying the finite element techniques to flexible mechanisms was performed by Winfrey [12,13], and Erdman, Sandor and Oakberg [14]. Following this trend, Bahgat and Willmert [15] also investigated this problem using the finite element method. While the deformation in axial direction is approximated by a linear polynomial, the transverse de-

[2]also known as gyroscopic damping matrix

flection is approximated by quintic polynomials which preserve moment compatibility between elements. The same quintic polynomials were also used by Cleghorn, Fenton and Tabarrok [16,17], and Cleghorn and Chao [18]. In addition to expressing the periodic forces and displacements in Equations (1.1) in terms of truncated Fourier series as in [15], Cleghorn et al. also expressed the global matrices in a similar manner. Dynamic strains for a four-bar mechanism were calculated. Good agreement with the experimental data presented in [19] was obtained.

Midha, Erdman and Frohrib [20−22] developed a systematic way to model elastic mechanisms using finite element techniques and a novel procedure to solve the resulting equations of motion. Later Turcic [23], and Turcic and Midha [24−26] addressed themselves to the development of a general finite element model using three dimensional elements. The equations of motion were presented, including all the extra acceleration terms except the pseudo-normal stiffness matrix. The modified iterative algorithm previously developed in [20,22] was utilized to solve the governing equations.

Nath and Ghosh [27,28] considered the motion-induced damping and stiffnesses in their formulation. To remove the singularity in the system matrices due to rigid body degree of freedom, a matrix decomposition method is employed. Steady state deflection of a slider-crank mechanism was favorably compared with that of Viscomi and Ayre [4].

Based upon the principle of virtual work, Thompson [29,30] devised a mathematical model for finite element analysis of high speed elastic machinery. Later the same author, together with Sung [31], developed a nonlinear finite element method for kineto-elastodynamic analysis of mechanisms. Geometric nonlinearity and the terms coupling the rigid body kinematics and elastic deformations are presented in their governing equations. The displacement predictions of an elastic slider-crank mechanism show good correlation with the measured data. Still using the above mathematical model, Sung et al. [32] presented a comprehensive experimental study on the kineto-elastodynamic responses of slider-crank mechanisms and four-bar linkages. Favorable correlation between the calculated deflections and experimental results was obtained.

Sunada and Dubowsky [33,34] investigated the vibrations of elastic spatial mechanisms by finite element method. The formulation was applied to an industrial manipulator in [34] and the calculated transfer functions were experimentally verified. More recently Bricout, Debus and Micheau [35] developed a finite element model for the dynamic analysis of spatial, multi-link, open-loop mechanisms. The equations of motion were solved using a single step algorithm developed by Zienkiewicz et al. [36] and Wood [37].

Apart from the continuum model in kineto-elastodynamic analysis of mechanisms, lumped parameter approach was also employed. Examples of

such analysis are found in [38−41].

Despite the numerous investigations on forced kineto-elastovibrations of mechanisms using both analytical and numerical methods, it is not very clear whether or when the motion-induced damping and stiffnesses can be neglected. This lack of understanding has resulted in, for example, the neglect of Coriolis and tangential accelerations. This is not all together surprising since the inclusion of these terms leads to the presence of non-proportional damping and asymmetric stiffness matrix, and thus results in complex eigensolutions. Examples of such analysis are presented in references [3,25,27], where these extra acceleration terms, although included in their formulation, are neglected in the final analysis. Another term that has been routinely ignored is the pseudo-normal acceleration term. This term arises from the axial foreshortening effects due to the transverse deflection. Neglect of this term yields incorrect solutions as it leads to the prediction of motion instability with increasing speeds, which is contrary to the expectation of increasing stability at high speeds. Such neglect is evident in some early publications [15,20,38,39,42]. Still others neglected the effects of all the extra acceleration terms [12,14,43,44]. The resulting equations of motion are still dynamic ones, but of the following form,

$$[M]\{\ddot{q}\} + [K_s]\{q\} = \{F\} \tag{1.3}$$

Although Viscomi and Ayre [4], and Thompson and Sung [31] considered

all the extra acceleration terms in their equations of motion, they did not specifically investigate the influence of these terms on the response of the system. Cleghorn, Fenton and Tabarrok [16] also considered these extra terms, but no solution algorithm was presented for determining the complex eigensolutions.

As has been outlined above, majority of the work is focused upon the solution of system response. Only a few of them presented some results on the free vibration characteristics of elastic mechanisms. Kalaycioglu and Bagci [44], and Turcic and Midha [25] studied the natural frequencies of elastic mechanisms with all the extra acceleration terms ignored. In fact, the natural frequencies they obtained are merely those of a structure at different configurations governed by Equations (1.3). Based on this research work, Han, Zu and Xu [45] formulated the problem with all the extra acceleration terms considered. They also presented the axial foreshortening effect by a kinetic energy approach. A thorough investigation into the effects of the extra acceleration terms on the free vibration characteristics of a crank-rocker mechanism is presented in references [46,47].

1.2 Research Scope

As pointed earlier, numerous work on forced vibration analysis of flexible mechanisms has been presented. However, little work has been done in the

free vibration analysis of elastic mechanisms, especially when the extra acceleration terms are considered. The purpose of this research is to address the lack of comprehensive study of how these extra acceleration terms influence the free vibration characteristics of elastic mechanisms, especially during high speed operations. Finite element approach will be employed to formulate the problem.

The balance of this thesis is divided into three chapters with

- **Chapter 2** Derivation of the equations of motion by finite element method via Lagrange's equation. Systematic representations of the motion-induced influence, namely the Coriolis damping matrix, tangential, normal and pseudo-normal stiffness matrices, are presented.
- **Chapter 3** Free vibration analysis of flexible mechanisms. The influence of the extra acceleration terms on the dynamic characteristics of the system is investigated.
- **Chapter 4** Conclusions and recommendations.
- **Appendix A** List of element matrices.
- **Appendix B** User's manual for program FKEV.
- **Appendix C** Program for free kineto-elastovibration analysis.

Chapter 2

Formulation

2.1 Introduction

The equations of motion governing flexible mechanisms are derived and presented in this chapter. Displacement finite element method is employed to formulate the governing equations. It involves representing the flexible mechanism, assumed to be operating at a constant input velocity, by a moving frame. At every instant of the periodic motion, the rigid body configuration of the mechanism is treated as an *instantaneous structure* formed by a series of Euler-Bernoulli beam elements. Each moving member of the mechanism is discretized by as many finite elements as desired for accuracy. Both transverse and longitudinal deflections are taken into account in the finite element analysis.

The absolute motion of each finite element is decomposed into a rigid body displacement and an elastic deformation measured in a moving coordinate

system fixed on the element in its undeformed state. It is assumed that the vibrations of the mechanism are caused by the mechanism's own inertia only, and that no structural damping exists in the system. Due to the presence of the driving torque on the input crank, it behaves as a rotating cantilever beam.

2.2 Derivation of Element Matrices

2.2.1 Kinetic Energy of Element

Figure 2.1 shows a general flexible beam element governed by the Euler-Bernoulli beam theory in two corresponding configurations, namely the deformed and undeformed configurations. Elastic deflections of the element in transverse and longitudinal directions are superimposed upon the prescribed rigid body motions. The equations of motion are derived in their most general form using Lagrange's equation. Coriolis, tangential, normal and pseudo-normal acceleration components of elastic deformations are clearly identified in the formulation.

Three frames of reference are adopted in the analysis, as shown in Figure 2.1. The first is the inertia or global coordinate system, represented by OXY with its origin arbitrarily located. The second is another global coordinate system, Oxy with the origin at the same point. The last one, $o\xi\eta$ is the element-oriented coordinate system or the local coordinate system, whose

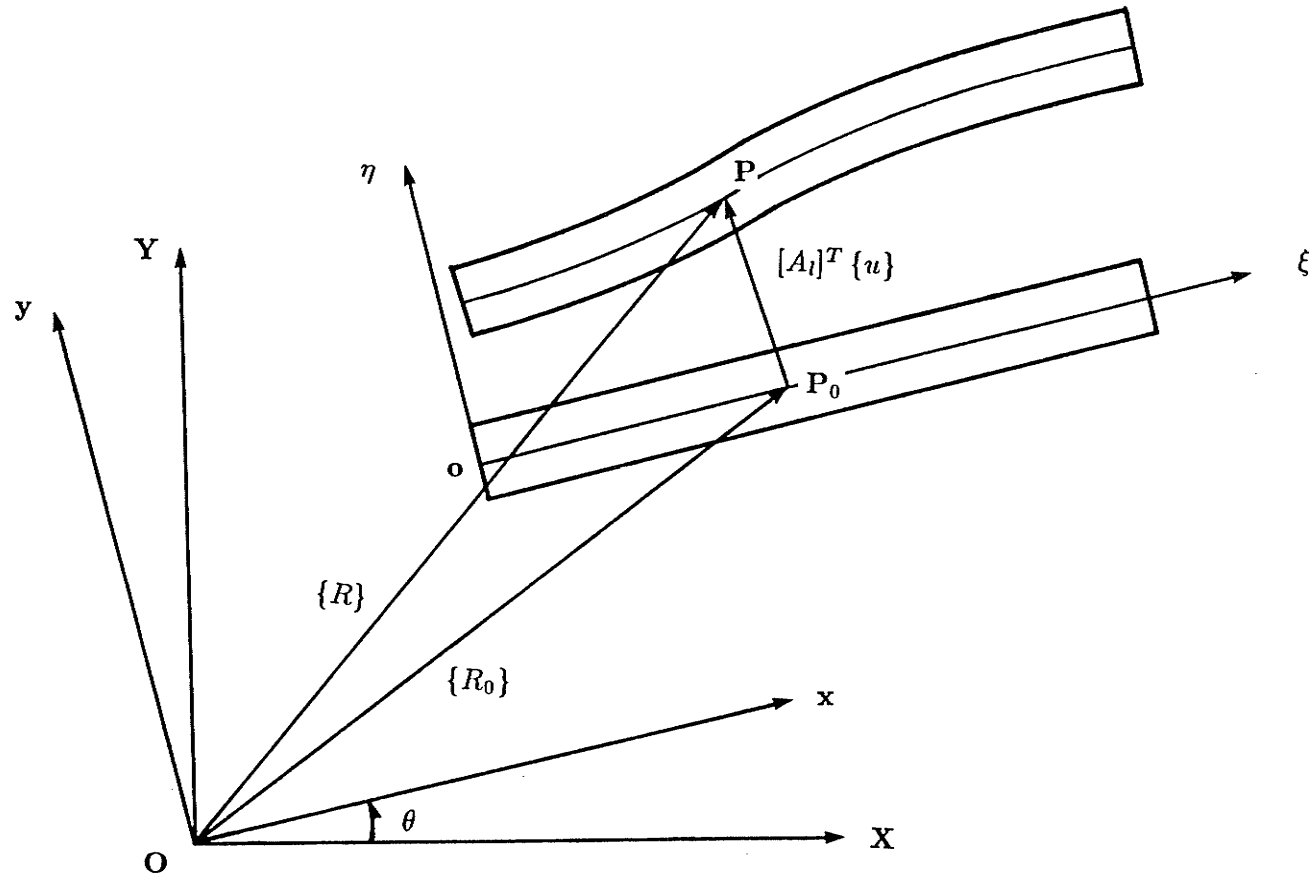

Figure 2.1: A general beam element at the undeformed and deformed configurations depicted in the associated coordinate systems

origin is at the left hand end of the element as depicted. The difference between OXY and Oxy lies in the fact that the latter is a rotating system, which is so selected that the x-axis keeps parallel to the center-line of the beam element.

The displacement vector expressed in $o\xi\eta$ coordinate system is given by

$$\{u\} = \left\{ \begin{array}{c} u(\xi,t) \\ v(\xi,t) \end{array} \right\} = [N]\{q_e\} \tag{2.1}$$

where $u(\xi,t)$ and $v(\xi,t)$ represent the longitudinal and transverse deflections at any point within the element, respectively, and $[N]$ is the shape function matrix and $\{q_e\}$ is the element nodal quantity vector. These latter two matrices are given by

$$[N] = \left[\begin{array}{cccccc} N_1 & 0 & 0 & N_4 & 0 & 0 \\ 0 & N_2 & N_3 & 0 & N_5 & N_6 \end{array} \right] \tag{2.2}$$

and

$$\{q_e\} = \left\{ \begin{array}{c} u_1 \\ v_1 \\ \Omega_1 \\ u_2 \\ v_2 \\ \Omega_2 \end{array} \right\} \tag{2.3}$$

in which,

$$\begin{aligned} N_1 &= 1-\zeta \\ N_2 &= 3(1-\zeta)^2 - 2(1-\zeta)^3 \end{aligned}$$

$$
\begin{aligned}
N_3 &= l\zeta(1-\zeta)^2 \\
N_4 &= \zeta \\
N_5 &= 3\zeta^2 - 2\zeta^3 \\
N_6 &= -l\zeta^2(1-\zeta)
\end{aligned}
$$

where $\zeta = \xi/l$ and l is the length of the element.

It should be pointed out that the selection of the shape functions is not unique and can be based on a number of different theories and approximations depending upon the characteristics of the particular problem to be analysed. However, to obtain monotonic convergence of the finite element solution, as the number of elements in the analysis increases, the shape functions must satisfy the following requirements:

1. The functions must be continuous within the element and across the element boundaries when the element is joined to other elements. This is necessary to ensure that the displacement functions will also be continuous.

2. The assumed functions must be able to represent constant (including zero) values of relevant strains and stresses. A consequence of this requirement ensures zero strains within the element for rigid body displacement mode.

3. The shape functions must satisfy the compatibility conditions between

elements.

Once the shape functions have been selected, the strains and stresses within the element can be determined as functions of the nodal quantity vector $\{q_e\}$.

Let $\{R\}$ and $\{R_0\}$ be the position vectors of deformed and undeformed positions of point P, measured in OXY coordinate system. Then, $\{R\}$ can be expressed as

$$\{R\} = \{R_0\} + [A_l]^T\{u\} \tag{2.4}$$

where $[A_l]$ is the transformation matrix from global coordinate to local coordinate, given by

$$[A_l] = \begin{bmatrix} \cos\theta & \sin\theta \\ -\sin\theta & \cos\theta \end{bmatrix}$$

Substituting Equations (2.1) into Equations (2.4) yields the following,

$$\{R\} = \{R_0\} + [A_l]^T[N]\{q_e\} \tag{2.5}$$

The velocity at point P of the element is given by differentiating Equations (2.5) with respect to time, i.e.

$$\{\dot{R}\} = \{\dot{R}_0\} + [\dot{A}_l]^T[N]\{q_e\} + [A_l]^T[N]\{\dot{q}_e\} \tag{2.6}$$

Thus, the kinetic energy of the element can be obtained from

$$T_e = \frac{1}{2}\int_0^l \rho A\{\dot{R}\}^T\{\dot{R}\}d\xi \tag{2.7}$$

where ρ is the mass density, A the cross sectional area of the element, and $(\dot{})$ denotes the time derivative. Substituting Equations (2.6) into Equation (2.7) yields,

$$\begin{aligned} T_e &= \frac{1}{2}\int_0^l \rho A \Big(\{\dot{R}_0\}^T\{\dot{R}_0\} + 2\{\dot{R}_0\}^T[\dot{A}_l]^T[N]\{q_e\} \\ &\quad +2\{\dot{R}_0\}^T[A_l]^T[N]\{\dot{q}_e\} + \{q_e\}^T[N]^T[\dot{A}_l][\dot{A}_l]^T[N]\{q_e\} \\ &\quad +2\{q_e\}^T[N]^T[\dot{A}_l][A_l]^T[N]\{\dot{q}_e\} \\ &\quad +\{\dot{q}_e\}^T[N]^T[A_l][A_l]^T[N]\{\dot{q}_e\}\Big)\, d\xi \end{aligned} \tag{2.8}$$

Noting that

$$[A_l][A_l]^T = [I]$$

$$[\dot{A}_l][\dot{A}_l]^T = \dot{\theta}^2[I]$$

and

$$[A_l][\dot{A}_l]^T = \dot{\theta}\begin{bmatrix} 0 & -1 \\ 1 & 0 \end{bmatrix}$$

Equation (2.8) becomes

$$\begin{aligned} T_e &= \frac{1}{2}\{\dot{q}_e\}^T[m_e]\{\dot{q}_e\} + \frac{\dot{\theta}^2}{2}\{q_e\}^T[m_e]\{q_e\} + \dot{\theta}\{\dot{q}_e\}^T[m_e^*]\{q_e\} \\ &\quad +\frac{1}{2}\int_0^l \rho A\{\dot{R}_0\}^T\{\dot{R}_0\}d\xi + \int_0^l \rho A\{\dot{R}_0\}^T[\dot{A}_l]^T[N]\{q_e\}d\xi \\ &\quad +\int_0^l \rho A\{\dot{R}_0\}^T[A_l]^T[N]\{\dot{q}_e\}d\xi \end{aligned} \tag{2.9}$$

where

$$[m_e] = \int_0^l \rho A[N]^T[N]d\xi \tag{2.10}$$

$$[m_e^\times] = \int_0^l \rho A[N]^T \begin{bmatrix} 0 & -1 \\ 1 & 0 \end{bmatrix} [N]d\xi \tag{2.11}$$

It is noticed that $[m_e]$ is the conventional symmetric mass matrix, and $[m_e^\times]$ is a skew-symmetric secondary mass matrix. Explicit expressions for both matrices are given in Appendix A. Further analysis shows that the inclusion of $[m_e^\times]$ will eventually result in the generation of the matrices associated with the Coriolis and tangential accelerations, both of which are considered here.

In order to obtain the element equations of motion by Lagrange's equation, the following manipulations are helpful.

$$\begin{aligned} \frac{d}{dt}\frac{\partial T_e}{\partial\{\dot{q}_e\}} &= [m_e]\{\ddot{q}_e\} + \dot{\theta}[m_e^\times]\{\dot{q}_e\} + \ddot{\theta}[m_e^\times]\{q_e\} \\ &\quad + \int_0^l \rho A[N]^T \left([\dot{A}_l]\{\dot{R}_0\} + [A_l]\{\ddot{R}_0\}\right) d\xi \end{aligned} \tag{2.12}$$

$$\frac{\partial T_e}{\partial\{q_e\}} = \dot{\theta}^2[m_e]\{q_e\} + \dot{\theta}[m_e^\times]\{\dot{q}_e\} + \int_0^l \rho A[N]^T[\dot{A}_l]\{\dot{R}_0\}d\xi \tag{2.13}$$

To evaluate the integrations in Equations (2.12) and (2.13), the rigid body velocity and acceleration are approximated by

$$\{\dot{R}_0\} = [A_l]^T[N]\{\dot{p}_0\} \tag{2.14}$$

$$\{\ddot{R}_0\} = [A_l]^T[N]\{\ddot{p}_0\} \tag{2.15}$$

where the vector $\{p_0\}$ is composed of the nodal coordinate components of rigid body configuration of the element, given by

$$\{p_0\} = \begin{Bmatrix} x_{10} \\ y_{10} \\ \theta \\ x_{20} \\ y_{20} \\ \theta \end{Bmatrix}$$

Substituting Equations (2.14) and (2.15) into Equations (2.12) and (2.13) yields,

$$\begin{aligned} \frac{d}{dt}\frac{\partial T_e}{\partial\{\dot{q}_e\}} &= [m_e]\{\ddot{q}_e\} + \dot{\theta}[m_e^*]\{\dot{q}_e\} + \ddot{\theta}[m_e^*]\{q_e\} \\ &\quad + \dot{\theta}[m_e^*]^T\{\dot{p}_0\} + [m_e]\{\ddot{p}_0\} \end{aligned} \tag{2.16}$$

$$\frac{\partial T_e}{\partial\{q_e\}} = \dot{\theta}^2[m_e]\{q_e\} + \dot{\theta}[m_e^*]^T\{\dot{q}_e\} + \dot{\theta}[m_e^*]^T\{\dot{p}_0\} \tag{2.17}$$

2.2.2 Strain Energy of Element

The strain energy of the element due to transverse and longitudinal deflections is given by

$$V_e = \frac{1}{2}\int_0^l \left\{EA[u'(\xi,t)]^2 + EI[v''(\xi,t)]^2\right\} d\xi \tag{2.18}$$

where E is the modulus of elasticity, I the area moment of inertia, $(\ )' = \frac{d(\ )}{d\xi}$ and $(\ )'' = \frac{d^2(\ )}{d\xi^2}$. The axial and transverse displacements are given respectively by

$$u(\xi,t) = u_1(t)N_1(\xi) + u_2(t)N_4(\xi) \tag{2.19}$$

$$\begin{aligned} v(\xi,t) &= v_1(t)N_2(\xi) + \Omega_1(t)N_3(\xi) \\ &\quad + v_2(t)N_5(\xi) + \Omega_2(t)N_6(\xi) \end{aligned} \tag{2.20}$$

Substituting Equations (2.19) and (2.20) into Equation (2.18) gives

$$V_e = \frac{1}{2}\{q_e\}^T[k_e^s]\{q_e\} \tag{2.21}$$

where $[k_e^s]$ is the structural stiffness matrix of the element, given by

$$[k_e^s] = \int_0^l [N^\kappa]^T \begin{bmatrix} EA & 0 \\ 0 & EI \end{bmatrix} [N^\kappa] d\xi \tag{2.22}$$

in which,

$$[N^\kappa] = \begin{bmatrix} N_1' & 0 & 0 & N_4' & 0 & 0 \\ 0 & N_2'' & N_3'' & 0 & N_5'' & N_6'' \end{bmatrix}$$

The explicit expression for $[k_e^s]$ is given in Appendix A.

2.2.3 Potential Energy due to Axial Force

The potential energy due to axial force, F_ξ in an element can be expressed as

$$W_e = \frac{1}{2}\int_0^l F_\xi \left(\frac{\partial v}{\partial \xi}\right)^2 d\xi \tag{2.23}$$

The axial force, F_ξ can be approximately determined via a static analysis of the element. It can be shown [16] that,

$$\begin{aligned} F_\xi &= F_r - \rho A \ddot{x}_{10}(l-\xi) + \frac{1}{2}\rho A \dot{\theta}^2 (l^2 - \xi^2) \\ &\quad - \int_\xi^l \rho A \ddot{u} d\xi \end{aligned} \tag{2.24}$$

where F_r is the external axial force applied at the right hand end of the element, and $\ddot{x}_{10}$ the absolute rigid body acceleration component in axial direction at the left hand end of the element. If there are no externally applied forces in the system, the right hand end force of the element is simply part of the actions from adjacent element. For small deformations as assumed in this analysis, F_r is computed based upon the original undeformed rigid body configuration.

It is observed that the last term in Equation (2.24) will result in nonlinear expression for W_e when Equations (2.23) and (2.24) are combined. The assumption of small deformations is invoked to justify the neglect of the nonlinear terms in W_e expression. Therefore, combining Equations (2.23)

and (2.24) and neglecting the nonlinear term yield,

$$W_e = \frac{1}{2}\{q_e\}^T[k_e^f]\{q_e\} \tag{2.25}$$

where

$$\begin{aligned}[k_e^f] &= \int_0^l F_\xi [N']^T \begin{bmatrix} 0 & 0 \\ 0 & 1 \end{bmatrix} [N'] d\xi \\ &= [k_e^{f1}] + [k_e^{f2}] + [k_e^{f3}] \end{aligned} \tag{2.26}$$

Expressions for $[k_e^{f1}]$, $[k_e^{f2}]$ and $[k_e^{f3}]$ are given in Appendix A.

2.2.4 Element Equations of Motion

The Lagrange's equation for an unconstraint element can be written as

$$\frac{d}{dt}\frac{\partial \mathcal{L}}{\partial \{\dot{q}_e\}} - \frac{\partial \mathcal{L}}{\partial \{q_e\}} = \{0\} \tag{2.27}$$

where the Lagrangian $\mathcal{L}$ is given by

$$\mathcal{L} = V_e - T_e + W_e \tag{2.28}$$

Substituting Equation (2.28), together with Equations (2.16), (2.17) , (2.21) and (2.25), into Equations (2.27) yields the element equations of motion,

$$[m_e]\{\ddot{q}_e\} + [c_e]\{\dot{q}_e\} + [k_e]\{q_e\} = \{f_e\} \tag{2.29}$$

where

$$[c_e] = 2\dot{\theta}[m_e^{\times}] \tag{2.30}$$

$$[k_e] = [k_e^s] + [k_e^t] + [k_e^n] + [k_e^f] \tag{2.31}$$

in which

$$[k_e^n] = -\dot{\theta}^2[m_e]$$

$$[k_e^t] = \ddot{\theta}[m_e^{\times}]$$

$$\{f_e\} = -[m_e]\{\ddot{p}_0\}$$

and $[k_e^s]$ is given by Equation (2.22), $[k_e^f]$ by Equation (2.26).

A detailed discussion of the damping matrix and the various stiffness matrices is now in order, to appreciate their respective contributions. Firstly, it is observed that the Coriolis damping matrix, $[c_e]$ is solely motion-induced, caused by the Coriolis components of elastic accelerations. Unfortunately, this is a non-proportional damping matrix and results in complex eigensolutions.

Secondly, the element stiffness matrix defined by Equation (2.31) comprises four component matrices. The structural stiffness matrix, $[k_e^s]$ is the usual stiffness matrix, composed of both bending and axial stiffnesses, and requires no further introduction. The other three component matrices are known as motion-induced stiffnesses as they are related to motion. The first

of these, $[k_e^t]$ is the tangential stiffness. The skew-symmetry of this matrix unfortunately destroys the symmetry of the overall stiffness matrix. Its presence is due only to the tangential components of elastic accelerations. This term, which is routinely ignored in many previous work, is often a necessary term as the tangential accelerations can have non-zero or even significant values in some parts during the motion of a mechanism even if the mechanism operates at a constant angular velocity, especially at high speed motions.

The remaining two component stiffness matrices in Equation (2.31) are symmetric and act in the axial direction. The first term, $[k_e^n]$ is due only to the normal components of elastic accelerations. At high speeds, its effects are quite significant, as will be shown in the next chapter, and should not be neglected. The last term, $[k_e^f]$ is given the name *pseudo-normal* stiffness matrix since the components of it are related to the normal acceleration components of elastic deformations of the member. Again, this term has been neglected in several early works on rotating flexible mechanisms and this results in the incorrect conclusion of instability for this type of motion.

It was shown in reference [45] that this pseudo-normal stiffness matrix is identical to that obtained from the kinetic energy representation of the axial foreshortening effect due to transverse deflection.

2.3 System Governing Equations

Once the element equations of motion are obtained, the system governing equations can be derived with the help of the global transformation matrix $[R]$, given by

$$[R] = \begin{bmatrix} \cos\theta & \sin\theta & 0 & 0 & 0 & 0 \\ -\sin\theta & \cos\theta & 0 & 0 & 0 & 0 \\ 0 & 0 & 1 & 0 & 0 & 0 \\ 0 & 0 & 0 & \cos\theta & \sin\theta & 0 \\ 0 & 0 & 0 & -\sin\theta & \cos\theta & 0 \\ 0 & 0 & 0 & 0 & 0 & 1 \end{bmatrix} \tag{2.32}$$

The element nodal quantities expressed in the global and local coordinate systems are related by the following equations,

$$\{q_e\} = [R]\{q_e^\times\} \tag{2.33}$$

$$\{\dot{q}_e\} = [R]\{\dot{q}_e^\times\} \tag{2.34}$$

$$\{\ddot{q}_e\} = [R]\{\ddot{q}_e^\times\} \tag{2.35}$$

where $\{q_e^\times\}$ is the nodal quantity vector expressed in global coordinate, given by

$$\{q_e^\times\} = \begin{Bmatrix} U_1 \\ V_1 \\ \Omega_1 \\ U_2 \\ V_2 \\ \Omega_2 \end{Bmatrix}$$

Substituting Equations (2.33)−(2.35) into Equations (2.29) and pre-multiplying the resulting equations by $[R]^T$ yield,

$$[m]\{\ddot{q}_e^*\} + [c]\{\dot{q}_e^*\} + [k]\{q_e^*\} = \{f\} \tag{2.36}$$

where

$$[m] = [R]^T[m_e][R]$$

$$[c] = [R]^T[c_e][R]$$

$$[k] = [R]^T[k_e][R]$$

$$\{f\} = [R]^T\{f_e\}$$

Thus the governing equations of the system can be obtained by applying superposition theory.

$$[M]\{\ddot{q}\} + [C]\{\dot{q}\} + [K]\{q\} = \{F\} \tag{2.37}$$

where

$$[M] = \sum_{i=1}^{m}[m]_i$$

$$[C] = \sum_{i=1}^{m}[c]_i$$

$$[K] = \sum_{i=1}^{m}[k]_i$$

$$\{F\} = \sum_{i=1}^{m}\{f\}_i$$

and $\{q\}$ is the nth order nodal quantity vector of the entire system, expressed in the inertia coordinate system, m represents the number of elements in the system. Solution of these equations of motion is discussed in the next chapter.

Chapter 3

Free Vibration Analysis

3.1 Introduction

Despite the numerous investigations on the kineto-elastodynamics of mechanisms using both analytical and numerical methods, there have hardly been published results on free vibration analysis of flexible mechanisms, especially when the extra acceleration terms of the Coriolis, tangential, normal and pseudo-normal accelerations, are taken into consideration. The purpose of this chapter is to study and comprehend how these extra acceleration terms influence the natural frequencies and mode shapes of mechanisms, especially during high speed motions. Both natural frequencies and mode shapes are presented with varying degree of simplifications. The following section deals with the solution technique of the free vibration problem.

3.2 Solution Scheme

The equations of motion governing the vibration problem are given by Equations (2.37) as follows,

$$[M]\{\ddot{q}\} + [C]\{\dot{q}\} + [K]\{q\} = \{F\} \tag{3.1}$$

where $[M], [C], [K], \{q\}$ and $\{F\}$ are defined in the previous chapter.

The governing equations for free vibration analysis are obtained when the right hand side of Equation (3.1) is set to zero, i.e.

$$[M]\{\ddot{q}\} + [C]\{\dot{q}\} + [K]\{q\} = \{0\} \tag{3.2}$$

Noticed that the damping matrix $[C]$ in Equations (3.2) is non-proportional and thus solution of these equations gives rise to complex eigenvalues and eigenvectors. Unlike proportionally damped linear systems, where the equations of motion for the system could be uncoupled by means of a normal coordinate transformation and then solved with no great difficulty, a system with non-proportional damping could not be solved by this conventional modal analysis method.

The solution scheme described here involves converting the n equations, defined by Equations (3.2), into a $2n$ equation system with real coefficient matrices. This is done as follows [48],

$$\begin{bmatrix} [0] & [M] \\ [M] & [C] \end{bmatrix} \begin{Bmatrix} \{\ddot{q}\} \\ \{\dot{q}\} \end{Bmatrix} + \begin{bmatrix} -[M] & [0] \\ [0] & [K] \end{bmatrix} \begin{Bmatrix} \{\dot{q}\} \\ \{q\} \end{Bmatrix} = \begin{Bmatrix} \{0\} \\ \{0\} \end{Bmatrix} \tag{3.3}$$

These equations are often referred to as the "reduced" form of Equations (3.2), and may be written as

$$[A]\{\dot{y}\} + [B]\{y\} = \{0\} \tag{3.4}$$

where

$$[A] = \begin{bmatrix} [0] & [M] \\ [M] & [C] \end{bmatrix}$$

$$[B] = \begin{bmatrix} -[M] & [0] \\ [0] & [K] \end{bmatrix}$$

and

$$\{y\} = \begin{Bmatrix} \{\dot{q}\} \\ \{q\} \end{Bmatrix}$$

Observe that both $[A]$ and $[B]$ are now real and of order $2n$. However, symmetry in these two matrices is destroyed due to the presence of the skew-symmetric Coriolis damping matrix and the non-symmetric stiffness matrix $[K]$. Solution of Equations (3.4) will be found in which the displacements and velocities have the form $e^{\nu t}$, namely

$$\{\dot{y}\} = \nu\{y\} \tag{3.5}$$

where ν is the complex eigenvalues of Equations (3.4).

Equations (3.4) is then written as follows in terms of the unknown quantity ν and unknown eigenvector $\{y\}$,

$$\nu[A]\{y\} = -[B]\{y\} \tag{3.6}$$

Thus the governing equations for free vibration analysis are

$$[L(\lambda)]\{y\} = \{0\} \tag{3.7}$$

where

$$[L(\lambda)] = [B]^{-1}[A] + \lambda[I]$$

$$\lambda = \frac{1}{\nu}$$

and $[I]$ is the identity matrix.

Evaluation of the determinant in Equations (3.7) leads to an equation of order $2n$ in λ. Solution of this equation, which is achieved using the QZ algorithm developed by Moler and Stewart [49], results in a set of $2n$ eigenvalues, namely $\lambda_1, \lambda_2, ..., \lambda_{2n}$. For a stable system, each of these roots will be either real and negative (for a critically damped or overdamped mode) or complex with a negative real part (for an underdamped mode) in conjugate pairs. This negative real part, β_k can be interpreted as the natural frequencies of the free vibration and is obtained from

$$\nu_k = \frac{1}{\lambda_k} = \alpha_k + i\beta_k \tag{3.8}$$

Corresponding to each eigenvalue, λ_k there exists an eigenvector, $\{y^{(k)}\}$ with $2n$ components. For distinct eigenvalues, the corresponding eigenvector is computed from the columns of the $2n$ by $2n$ adjoint matrix $[L(\lambda)]$. That is,

$$\left\{y^{(k)}\right\} = c_k \left\{J_{ij}(\lambda_k)\right\} = c_k \left\{J_{ij}^{(k)}\right\} \tag{3.9}$$

where $\{J_{ij}^k\}$ denotes any column of the adjoint matrix $[J_{ij}(\lambda_k)]$ and c_k is the proportionality constant.

A finite element program has been developed based on this proposed formulation and solution scheme. The QZ algorithm which is used for solving the complex eigenproblem is available in the IMSL[1] package.

3.3 Numerical Examples

The solution scheme outlined previously is first checked by comparing the computed solution with published results. Fairly good agreement was obtained.

The free vibration problem of Turcic and Midha [25] for a four-bar crank rocker mechanism is used to verify the solution scheme. Having assessed the accuracy of the proposed solution scheme, the effects of the extra acceleration terms on the eigenvalues and eigenvectors are studied using a four-bar linkage,

[1]International Mathematics and Statistics Library

where the motion-induced damping and stiffnesses are taken into account.

Since the focus of this analysis is to ascertain the effects of the extra acceleration terms on the free kineto-elastovibrations of the mechanism, several models with different degree of simplifications are analysed. These simplifications are summarized in Table 3.1.

To facilitate numerical simulations, the following non-dimensional parameters are introduced, namely

- non-dimensional natural frequency parameter, λ_i
- non-dimensional rotational speed parameter, α
- percentage error in natural frequency, ϵ

These are defined respectively as:

$$\begin{aligned} \lambda_i &= \frac{\omega_i^j}{\omega_1^0} \\ \alpha &= \frac{\Omega}{\omega_1^0} \\ \epsilon &= \frac{\omega_i^j - \omega_i^1}{\omega_i^1} \times 100\% \end{aligned}$$

where ω_i^j $(i = 1, 2, 3, ...;\ j = 0, 1, ..., 5)$ is the ith mode natural frequency for the jth case under consideration and Ω is the input angular velocity. The latter quantity is assumed to be constant.

Table 3.1: Simplification Indices

	Motion Index	Motion Type
case 0	j=0	non-rotating mechanism, namely a structure
case 1	j=1	full solution, that is all terms included
case 2	j=2	Coriolis damping matrix neglected
case 3	j=3	tangential stiffness matrix neglected
case 4	j=4	normal stiffness matrix neglected
case 5	j=5	pseudo-normal stiffness matrix neglected

Further details of the verification analysis and the results of subsequent investigation are presented in the following sections.

3.3.1 Verification Example

A four-bar crank rocker mechanism with lumped masses at the crank-coupler and coupler-follower junctions is used as an example for verifying the accuracy of the proposed formulation and solution scheme. A sketch of the mechanism is depicted in Figure 3.1 and its characteristics are listed in Table 3.2. This problem was suggested and solved by Turcic and Midha [25] for its free vibration solutions. In a manner similar to their investigation, the results here are computed for three finite element models of the mechanism. The first model is based on a three element discretization scheme, the second using a six element scheme, and the third, a nine element scheme. In all of these models, each moving member is discretized with one, two and three elements

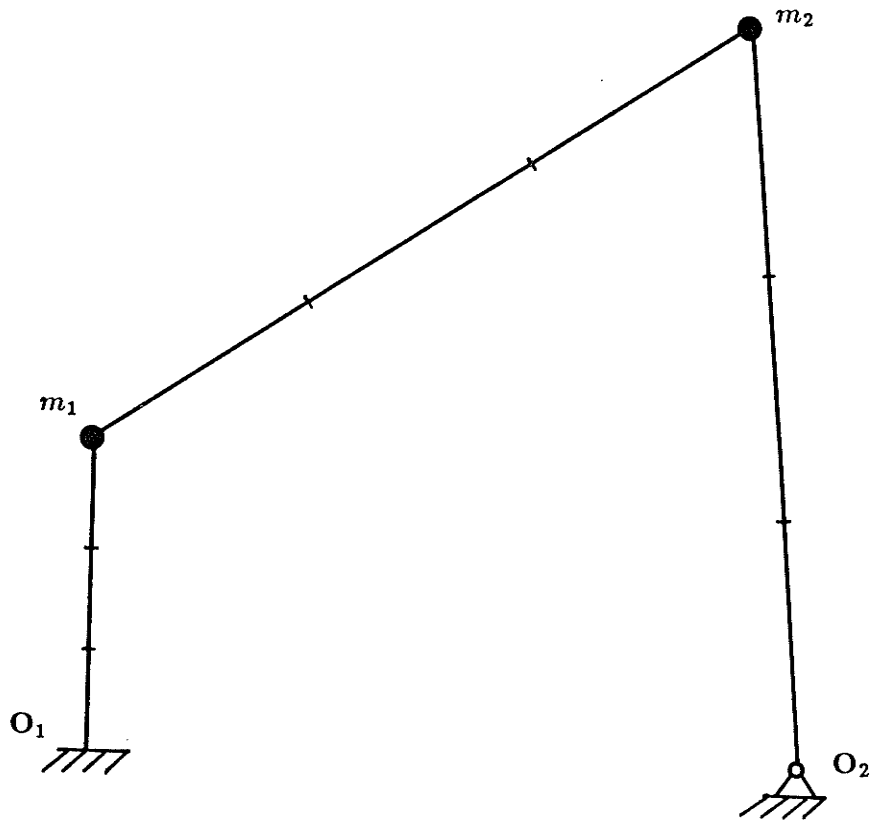

Figure 3.1: Finite element model 3 for the crank rocker mechanism[25]

Table 3.2: Characteristics of a Four-Bar Crank Rocker Mechanism [25]

	Length	Area	Moment of Inertia
Crank	10.80 cm (4.25 in)	1.07 cm^2 (0.17 in^2)	1.62×10^{-2} cm^4 (3.88×10^{-4} in^4)
Coupler	27.94 cm (11.00 in)	0.41 cm^2 (0.063 in^2)	8.67×10^{-4} cm^4 (2.08×10^{-5} in^4)
Follower	27.05 cm (10.65 in)	0.41 cm^2 (0.063 in^2)	8.67×10^{-4} cm^4 (2.08×10^{-5} in^4)
Distance between ground pivots, O_1O_2			25.40 cm (10.00 in)
Lumped mass of the bearing assembly at the crank-coupler junction, m_1			4.52×10^{-2} kg (2.53×10^{-4} slug)
Lumped mass of the bearing assembly at the coupler-follower junction, m_2			3.75×10^{-2} kg (2.53×10^{-4} slug)
Modulus of elasticity, E			7.1×10^7 kPa (1.03×10^7 psi)
Mass density, ρ			2.71×10^3 kg/m^3 (2.54×10^{-4} $slug/in^3$)

of equal lengths, respectively. All extra acceleration terms are neglected in this verification study and the mechanism is considered to be a static linkage or a structure, so as to be consistent with the results of [25]. Thus the governing equations for the free vibration analysis, as given by Equations (3.2), are reduced to:

$$[M]\{\ddot{q}\} + [K]\{q\} = \{0\} \tag{3.10}$$

where $[K]$ comprises only the structural stiffness matrix, namely both axial and bending stiffnesses. The variation of natural frequency with the crank angle for the first three modes are plotted in Figures 3.2−3.4. Exact comparison with the results of Turcic and Midha [25] is difficult since their solutions do not start precisely at $y-$axis. Thus their numerical values at 0° and 360° do not quite agree as they should. Nevertheless, the results obtained here are almost identical to those calculated by them.

3.3.2 A Rotating Four Bar Mechanism

Having evaluated the accuracy of the proposed formulation and the solution scheme, an investigation into the effects of the extra acceleration terms on the eigenvalues and eigenvectors with the mechanism operating at high speeds is now presented. A sketch of this mechanism, taken from Bahgat and Willmert [15], is depicted in Figure 3.5. Its geometric and material properties are listed in Table 3.3.

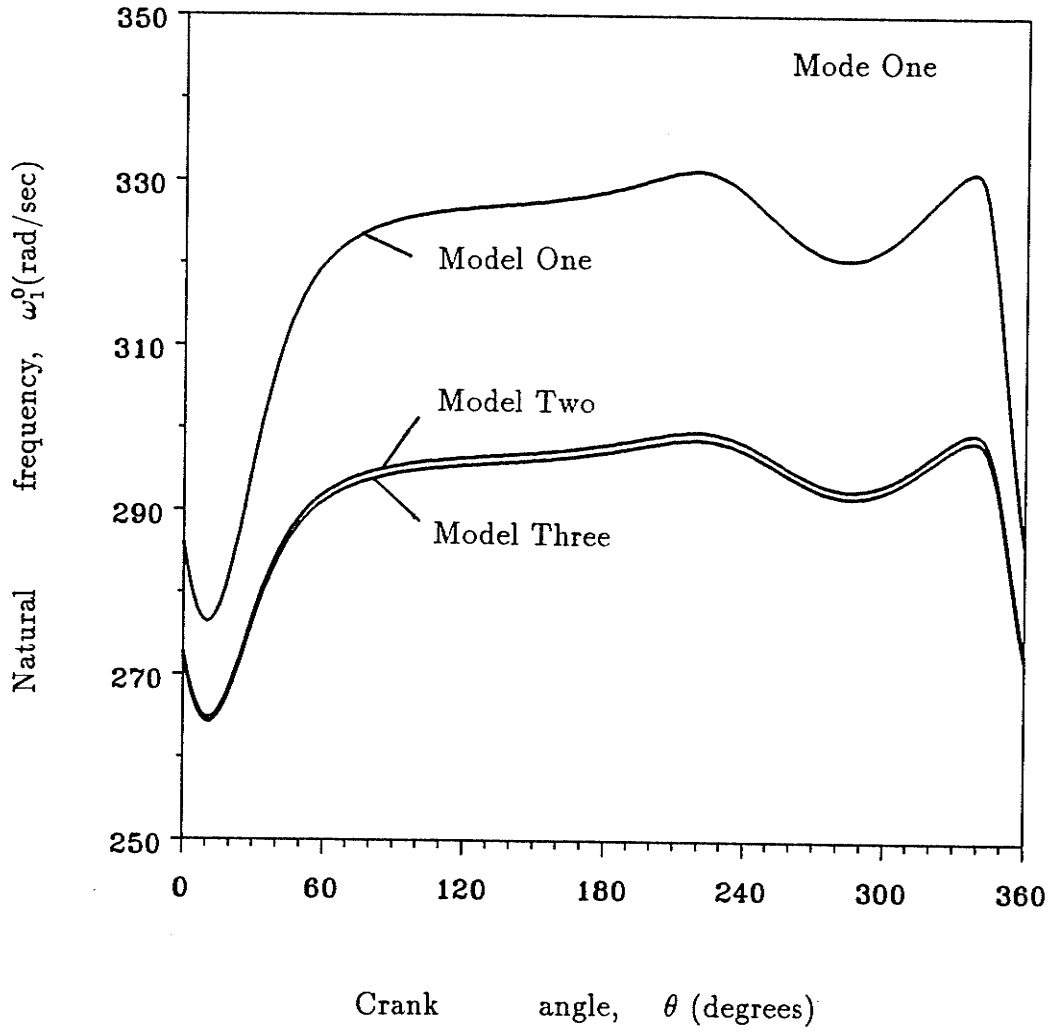

Figure 3.2: Natural frequency vs. crank angle

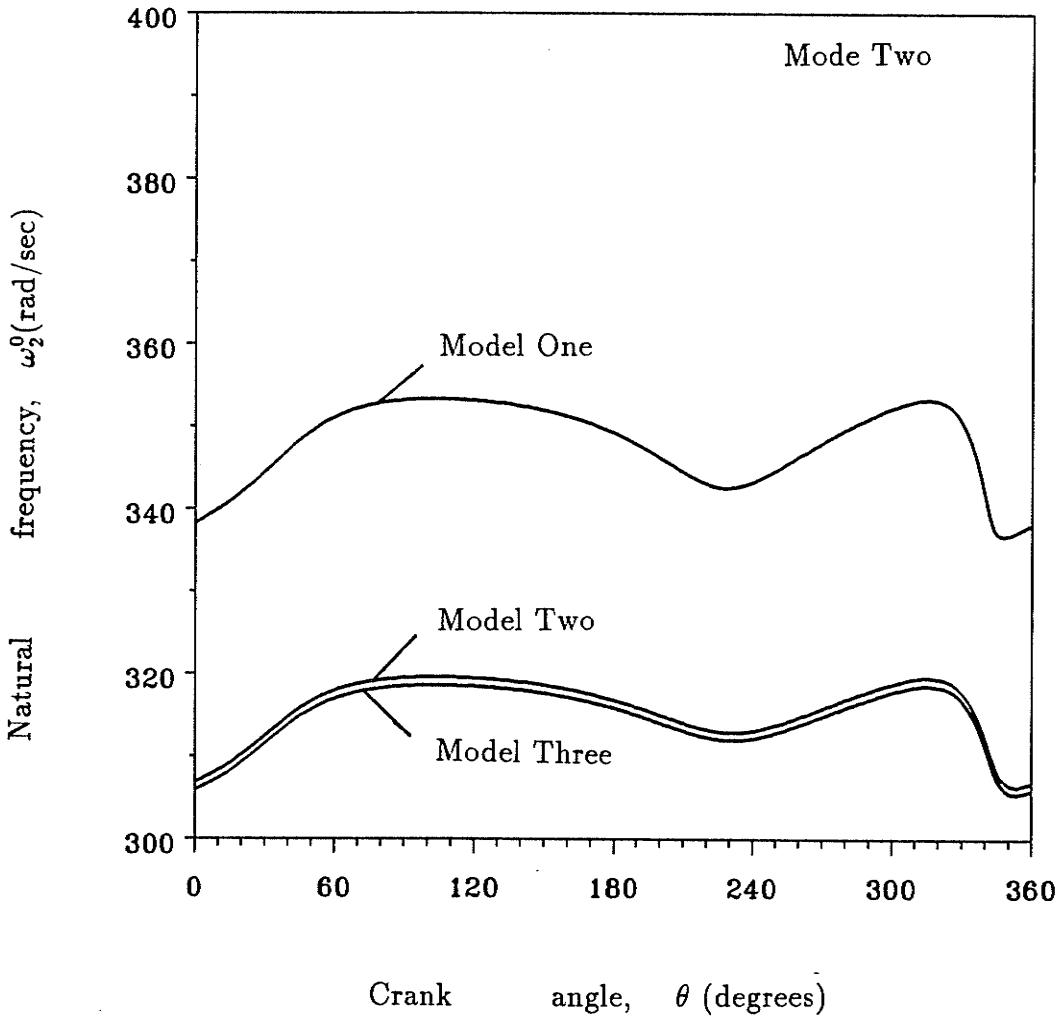

Figure 3.3: Natural frequency vs. crank angle

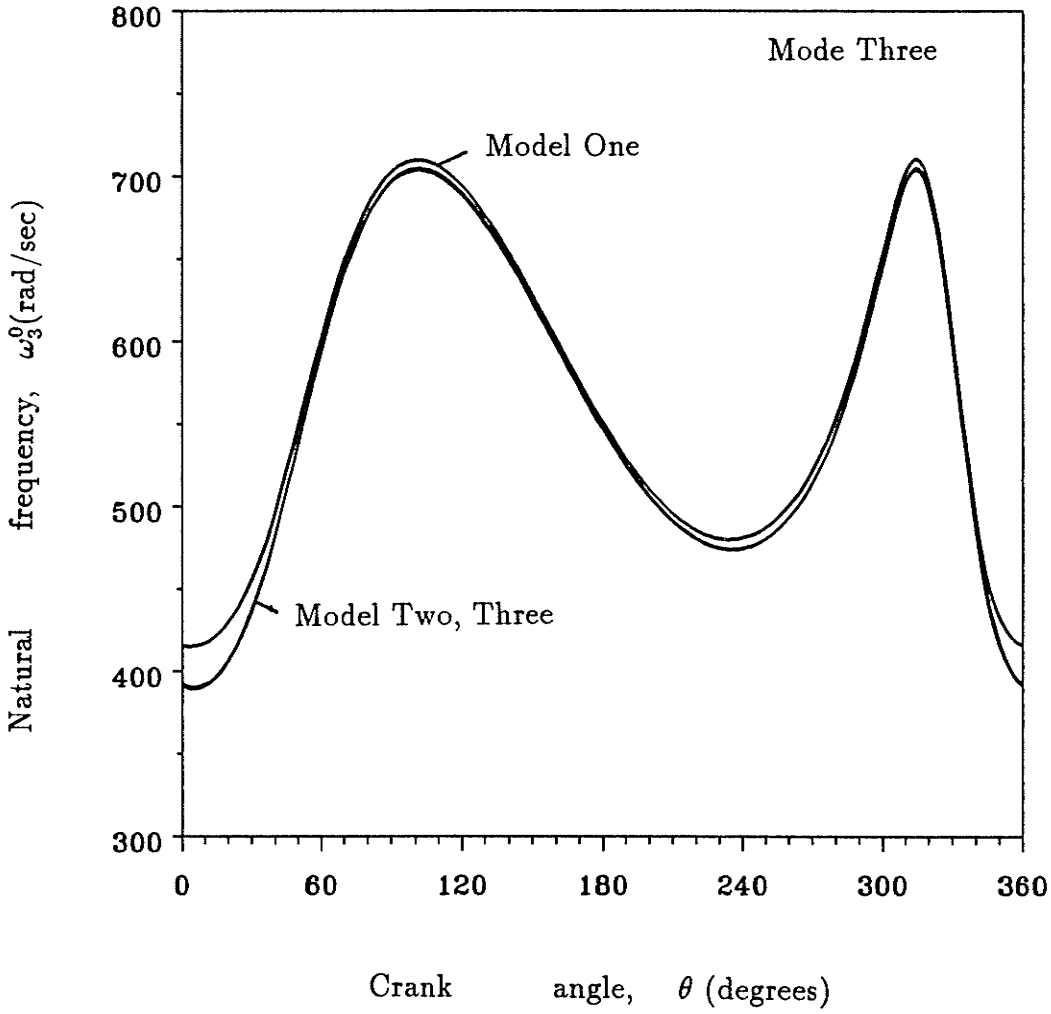

Figure 3.4: Natural frequency vs. crank angle

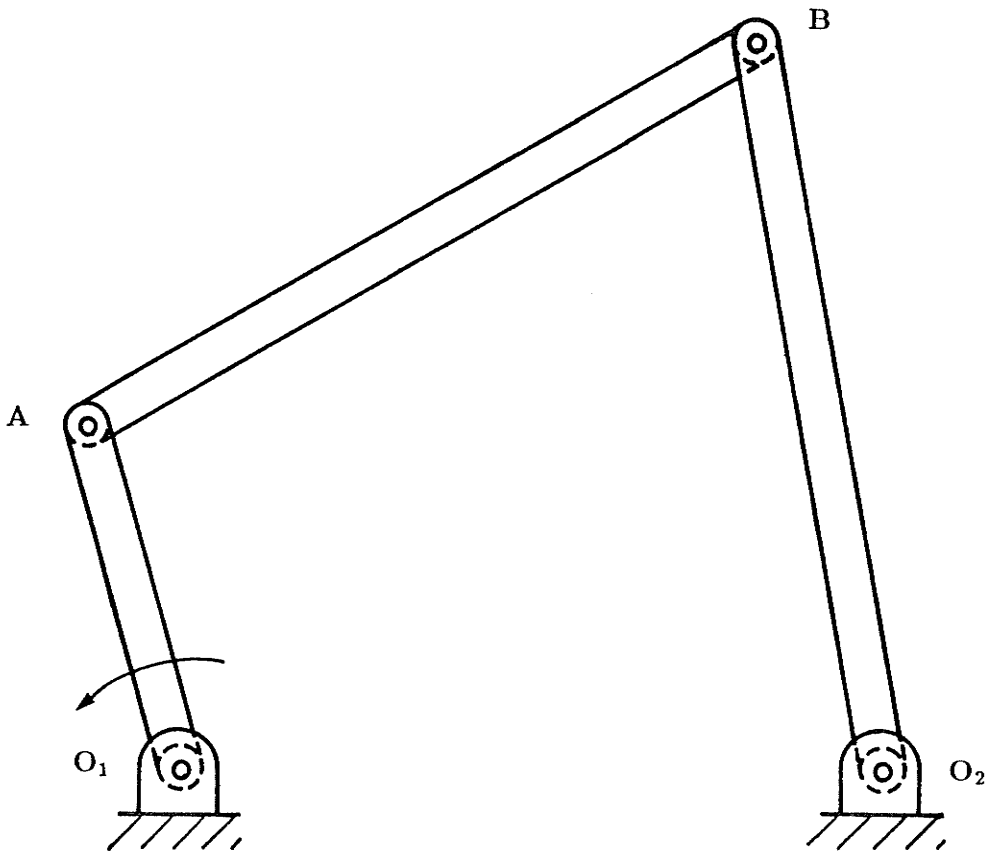

Figure 3.5: A general crank rocker mechanism [15]

Table 3.3: Characteristics of a Four-Bar Mechanism [15]

	Length	Area	Moment of Inertia
Crank	12.70 cm (5.00 in)	1.61 cm^2 (0.25 in^2)	8.66×10^{-1} cm^4 (2.08×10^{-2} in^4)
Coupler	27.94 cm (11.00 in)	1.61 cm^2 (0.25 in^2)	8.66×10^{-1} cm^4 (2.08×10^{-2} in^4)
Follower	26.67 cm (10.50 in)	1.61 cm^2 (0.25 in^2)	8.66×10^{-1} cm^4 (2.08×10^{-2} in^4)
Distance between ground pivots, O_1O_2			25.40 cm (10.00 in)
Modulus of elasticity, E			2.07×10^8 kPa (3.00×10^7 psi)
Mass density, ρ			7.76×10^3 kg/m^3 (7.25×10^{-4} $slug/in^3$)

Several finite element models with different discretization schemes have been investigated. Computational experience shows that the five element model, where the input crank is treated as one element and the coupler and follower are discretized into two elements each, gives reasonably accurate results. Therefore, only the results associated with this model will be presented.

Due to the change of geometry of the mechanism during motion, its natural frequencies vary as a function of the input parameters during a cycle of its motion. The dependence of natural frequencies on the gross motion (rigid body motion) defined by crank angle, θ is shown in Figures 3.6–3.9 for the

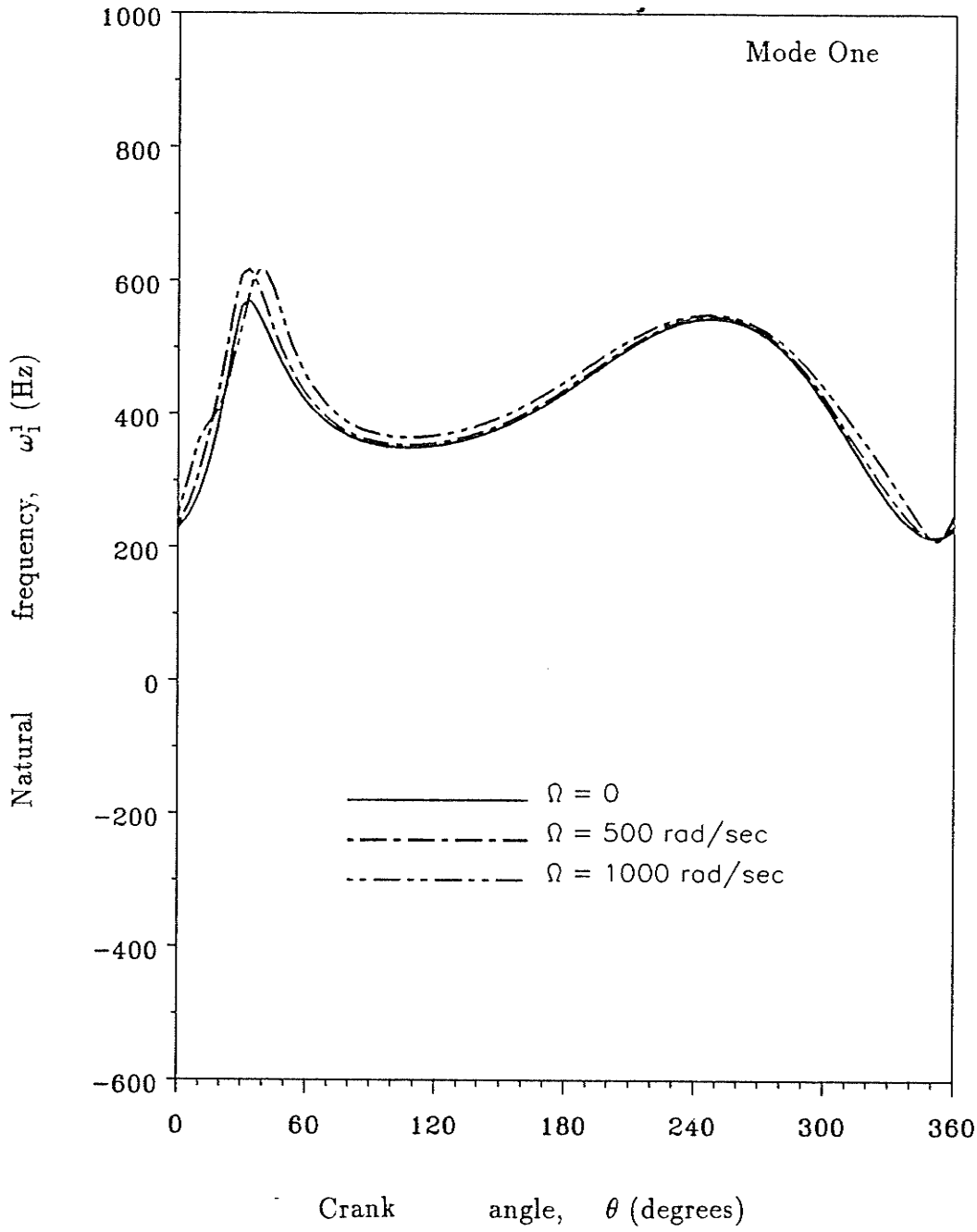

Figure 3.6: Natural frequency vs. crank angle

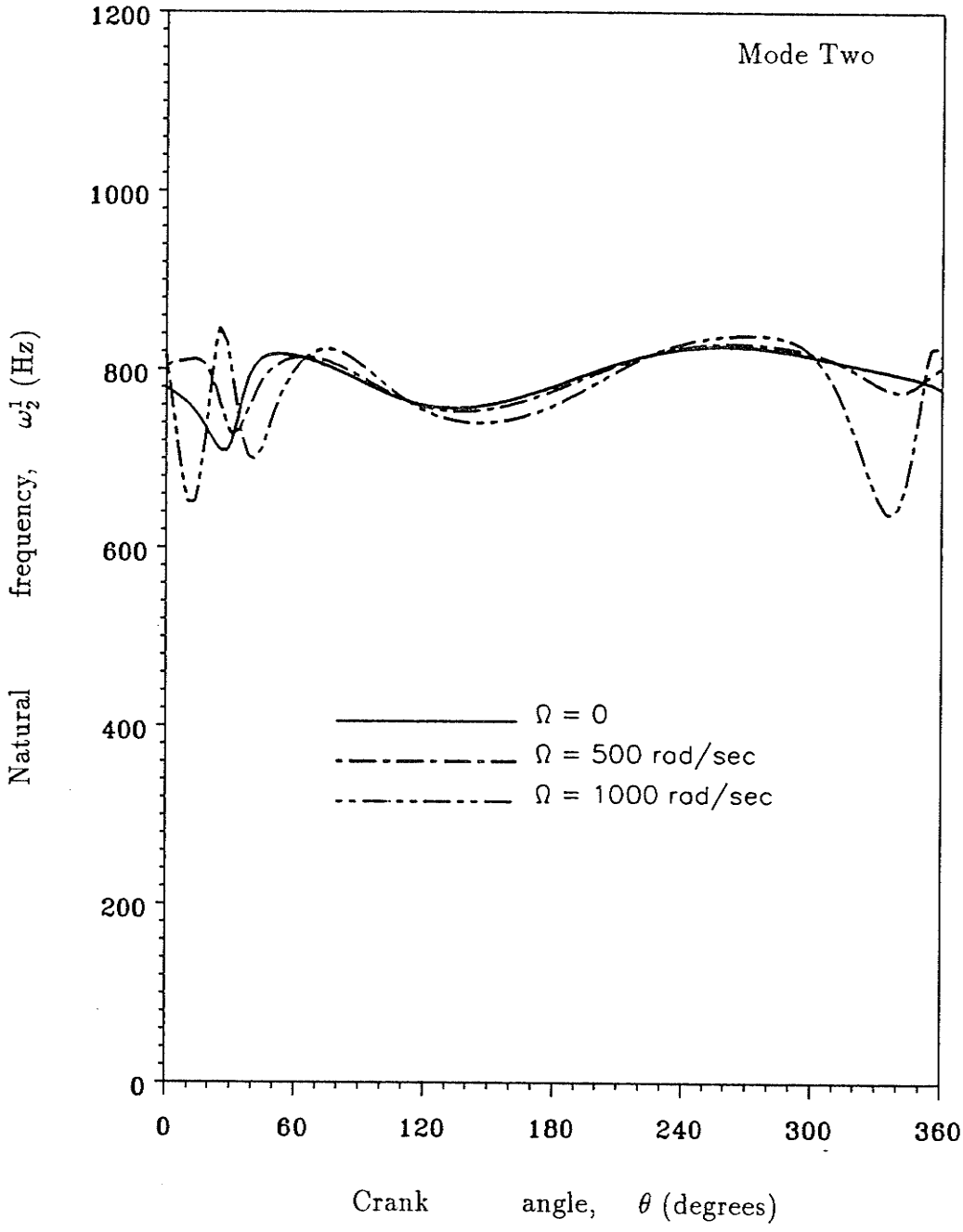

Figure 3.7: Natural frequency vs. crank angle

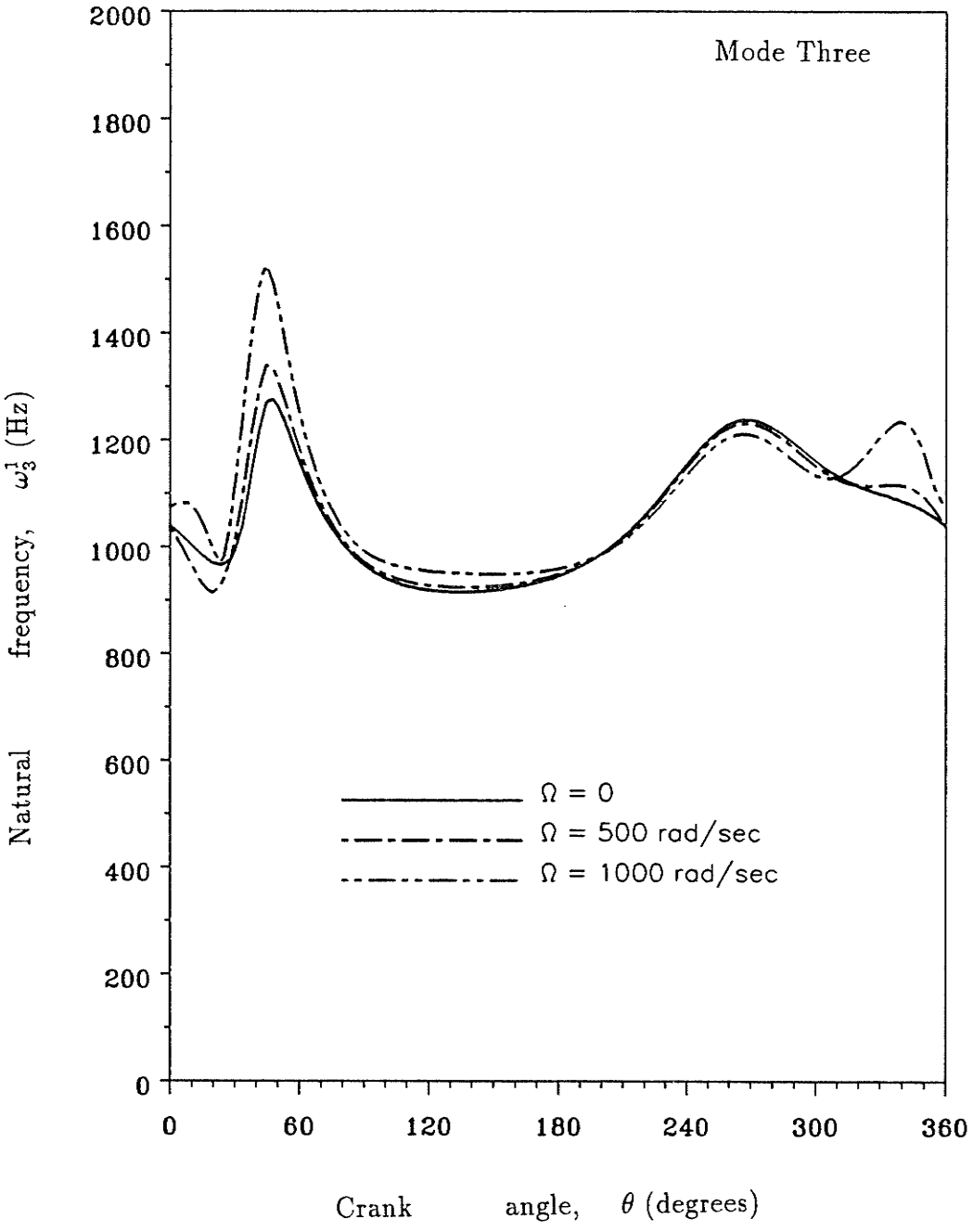

Figure 3.8: Natural frequency vs. crank angle

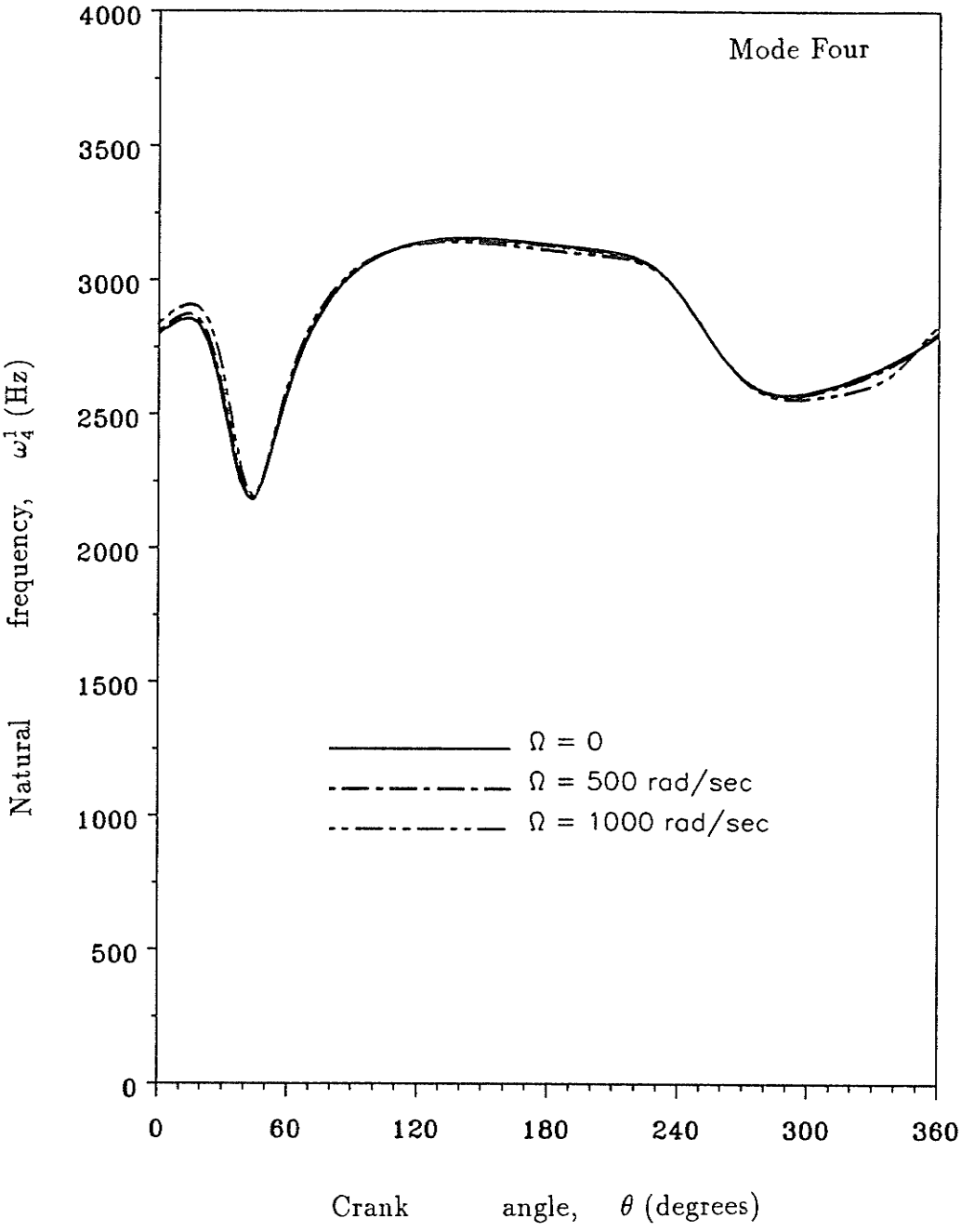

Figure 3.9: Natural frequency vs. crank angle

first four modes.

Only case 1 results are considered as the purpose here is to identify a region suitable for a more detailed analysis involving the effects of the extra acceleration terms. From these plots, it appears that the position around $\theta = 10°$ is one such desirable region. Observe also that each order of natural frequency experiences its minimum value at different locations as the mechanism moves through a cycle of its motion. The critical operating speed of a mechanism corresponding to its lowest natural frequency and the position at which this minimum natural frequency occurs, determines the critical geometry of the mechanism. As mentioned in [44], this critical geometry of a mechanism provides a very useful and economical tool for its elasto-dynamic design.

Figure 3.10−3.13 shows the variation of natural frequency parameters against input rotational speeds for cases $0-5$ at the position, $\theta = 10°$ for the first four modes. According to the definition of natural frequency parameter, the response curves for case 0 for all modes are horizontal lines. This is expected as the mechanism is now a stationary structure. The complete solution which includes solving for the complex eigenquantities is indicated by case 1. Solutions with varying degree of simplifications are denoted by cases $2-5$. Observe that at low operating speeds, for instance, $\alpha < 0.1$, the errors introduced by these approximations are very small. However, for high speed mechanisms, these errors can be significant, with the exception of case

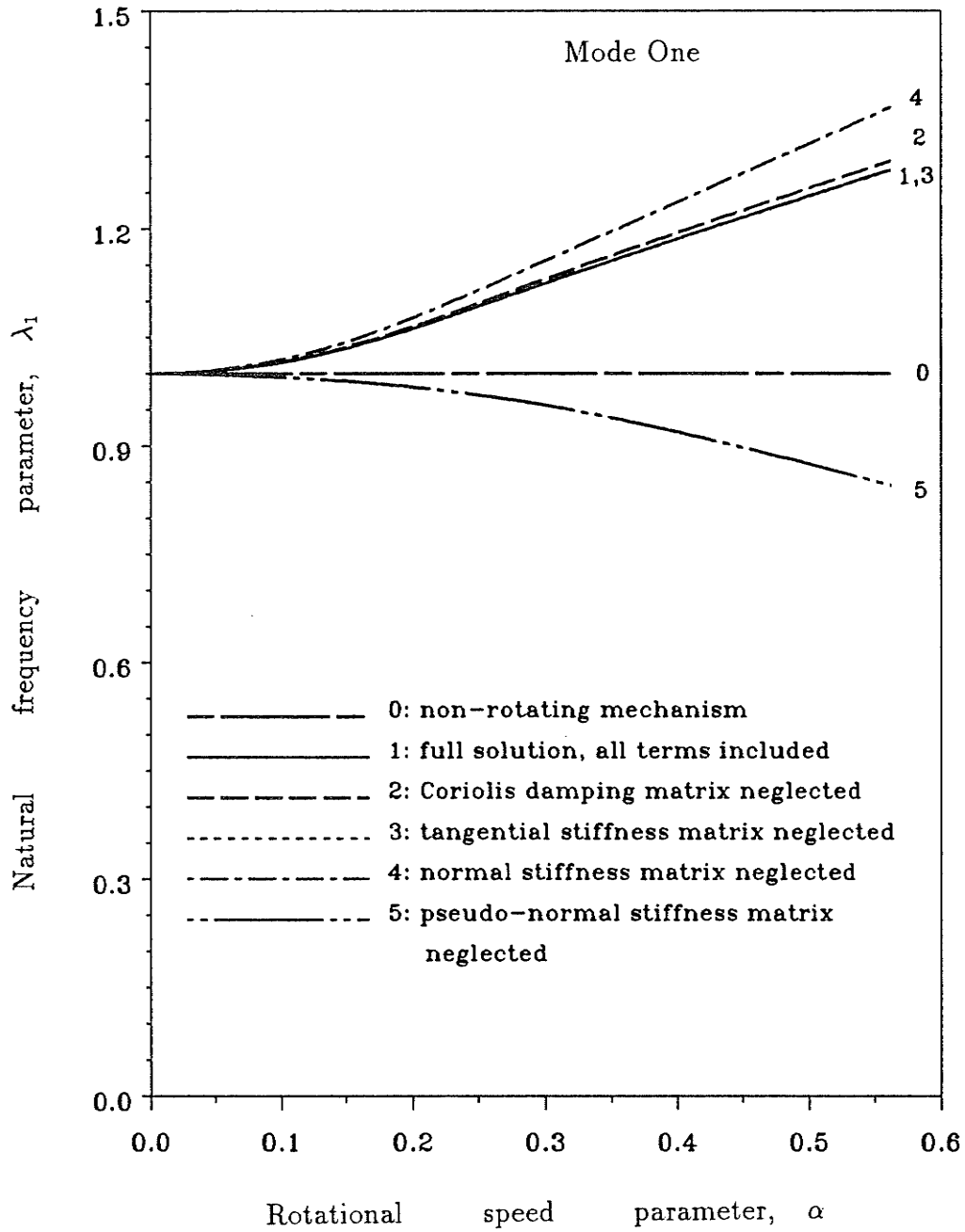

Figure 3.10: Natural frequency parameter vs. rotational speed parameter

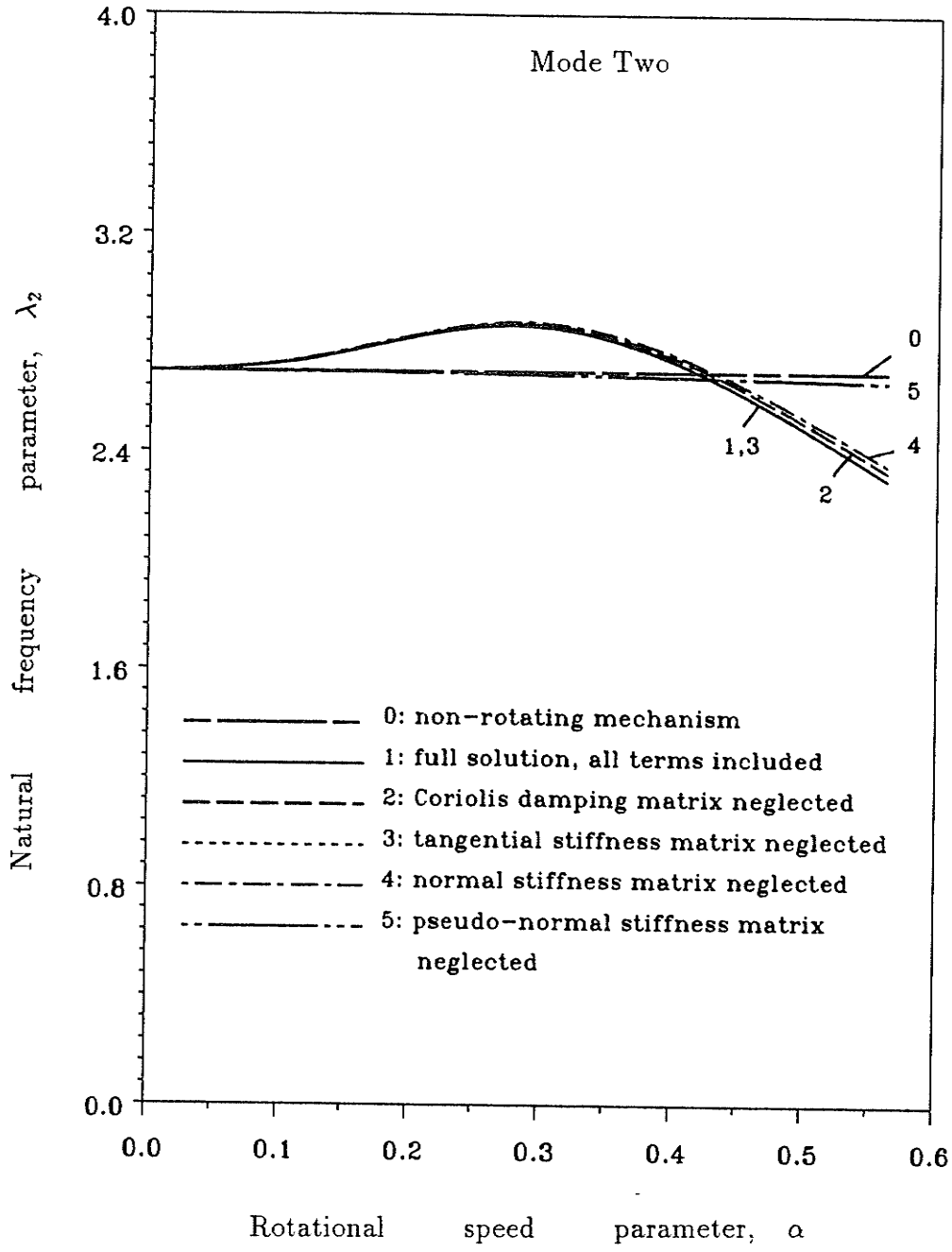

Figure 3.11: Natural frequency parameter vs. rotational speed parameter

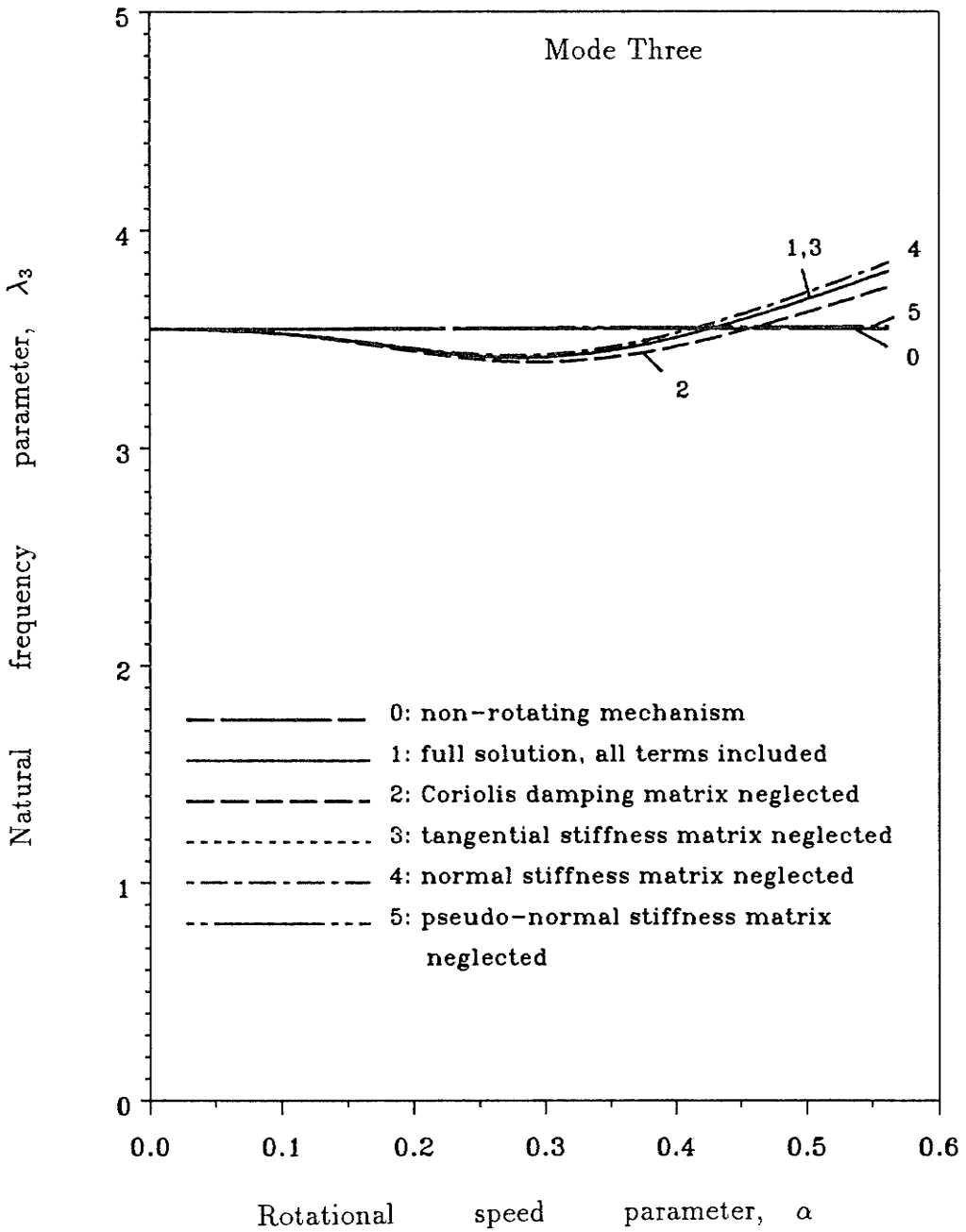

Figure 3.12: Natural frequency parameter vs. rotational speed parameter

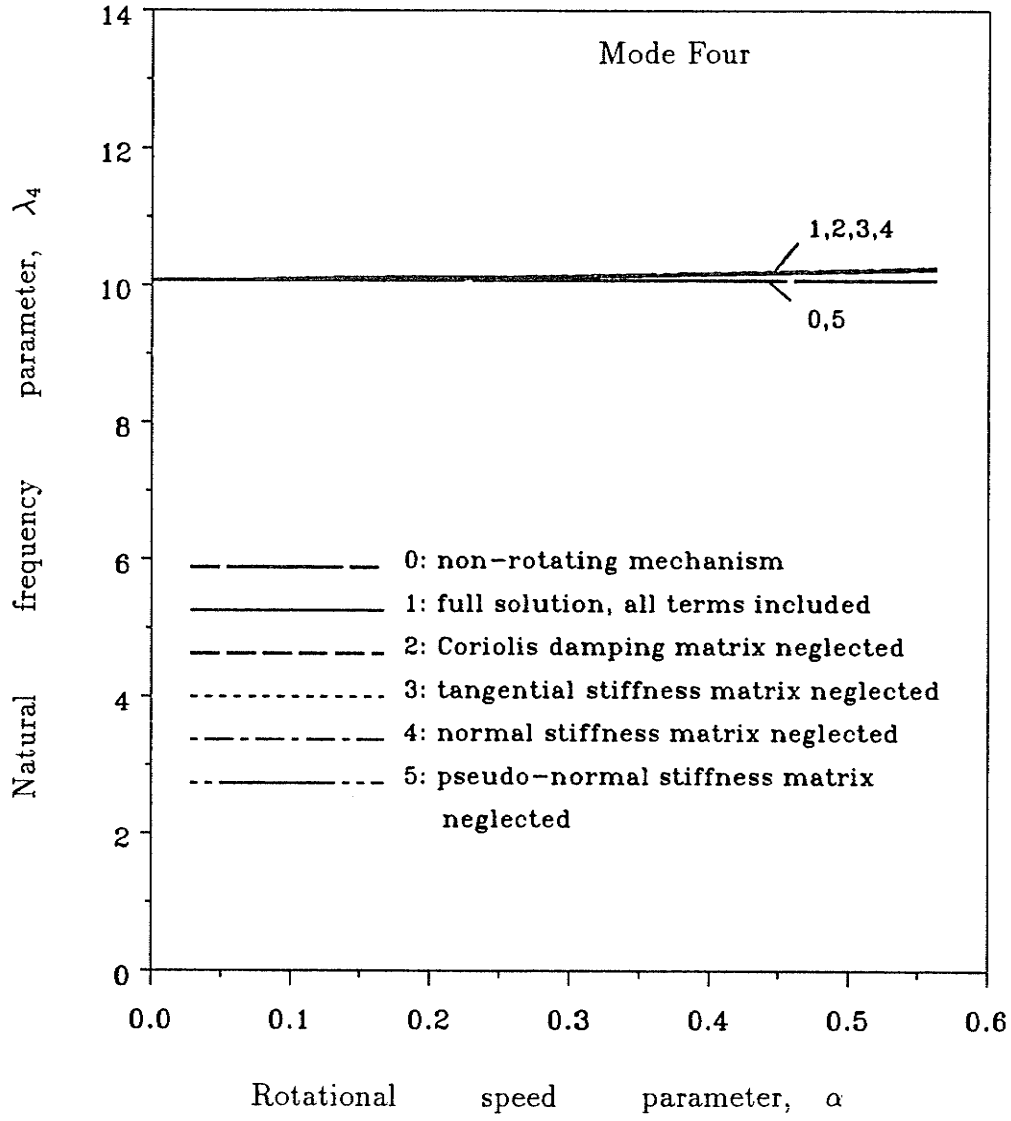

Figure 3.13: Natural frequency parameter vs. rotational speed parameter

2 and case 3 where the Coriolis damping matrix and the tangential stiffness matrix are neglected. In both situations, the simplified solutions match quite closely to the complete solution, namely case 1.

The error due to the neglect of the normal stiffness matrix increases with increasing speeds. In particular, the error in the fundamental mode frequency prediction at $\alpha = 0.56$ is approximately 8.5%. This set of graphs also reveals that the largest source of error is introduced by the neglect of the pseudo-normal stiffness matrix. Obviously, from the fundamental mode frequency response curve, incorrect results would be obtained if this term is dropped. The results should indicate increasing stability with increasing speeds, as the mechanism becomes stiffer and stiffer due to the increasing large axial forces. But when this term is neglected as was done by some researchers mentioned earlier, the results show increasing instability with increasing speeds, an error that was also noticed by Cleghorn et al. [16].

It will be interest to examine the distribution of the errors introduced by the neglect of the various motion-induced terms, that is, cases $2-5$, over an entire cycle of the motion for different operating speeds. This is depicted in the various plots given in Figures 3.14–3.17 for the first four modes, corresponding to $\Omega = 500$ rad/sec, and Figures 3.18–3.21 corresponding to $\Omega = 1000$ rad/sec. The $y-$axis shows a comparison of the percentage errors in natural frequencies computed by the various degree of simplifications with

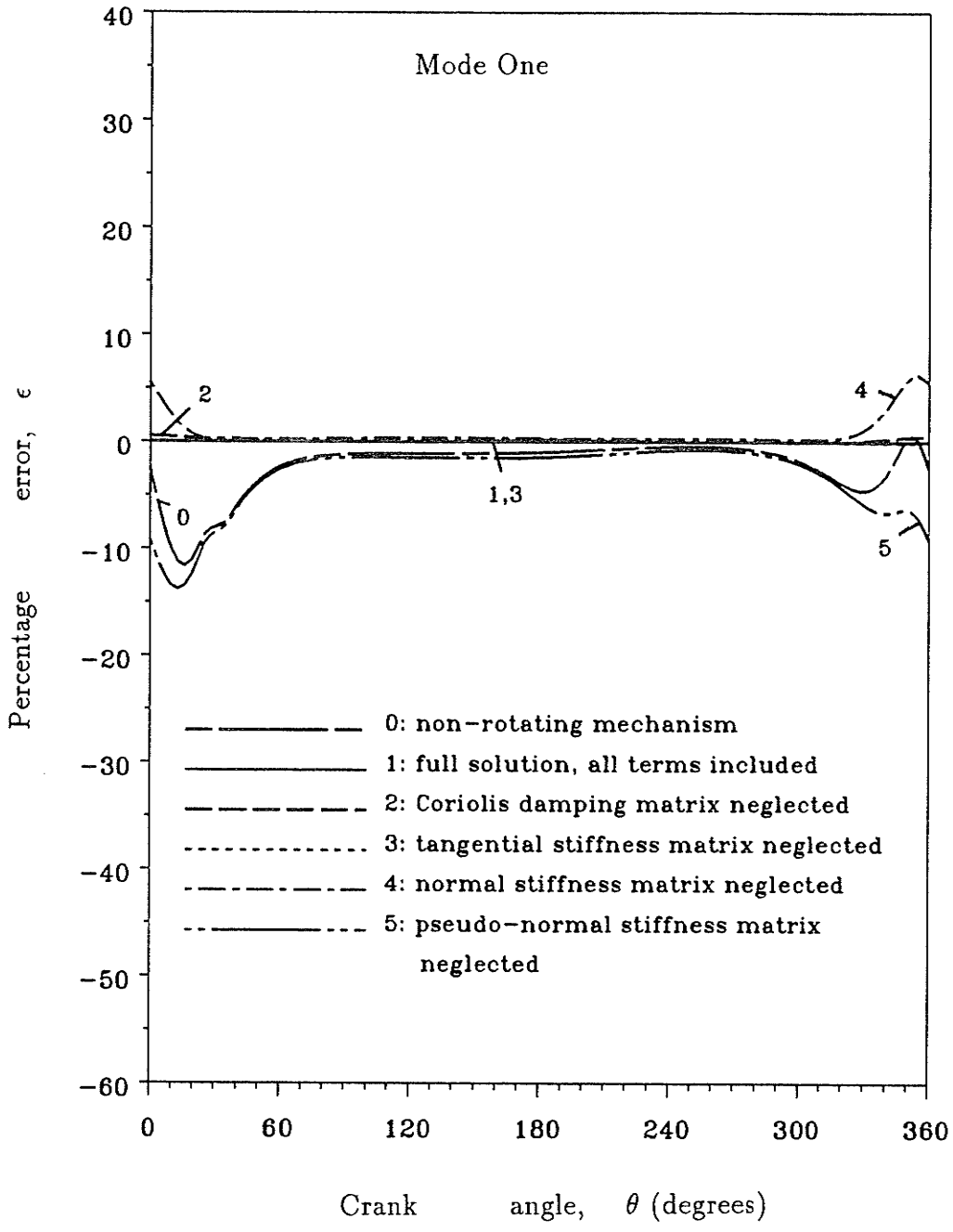

Figure 3.14: Percentage error in natural frequency vs. crank angle, Ω=500 rad/sec

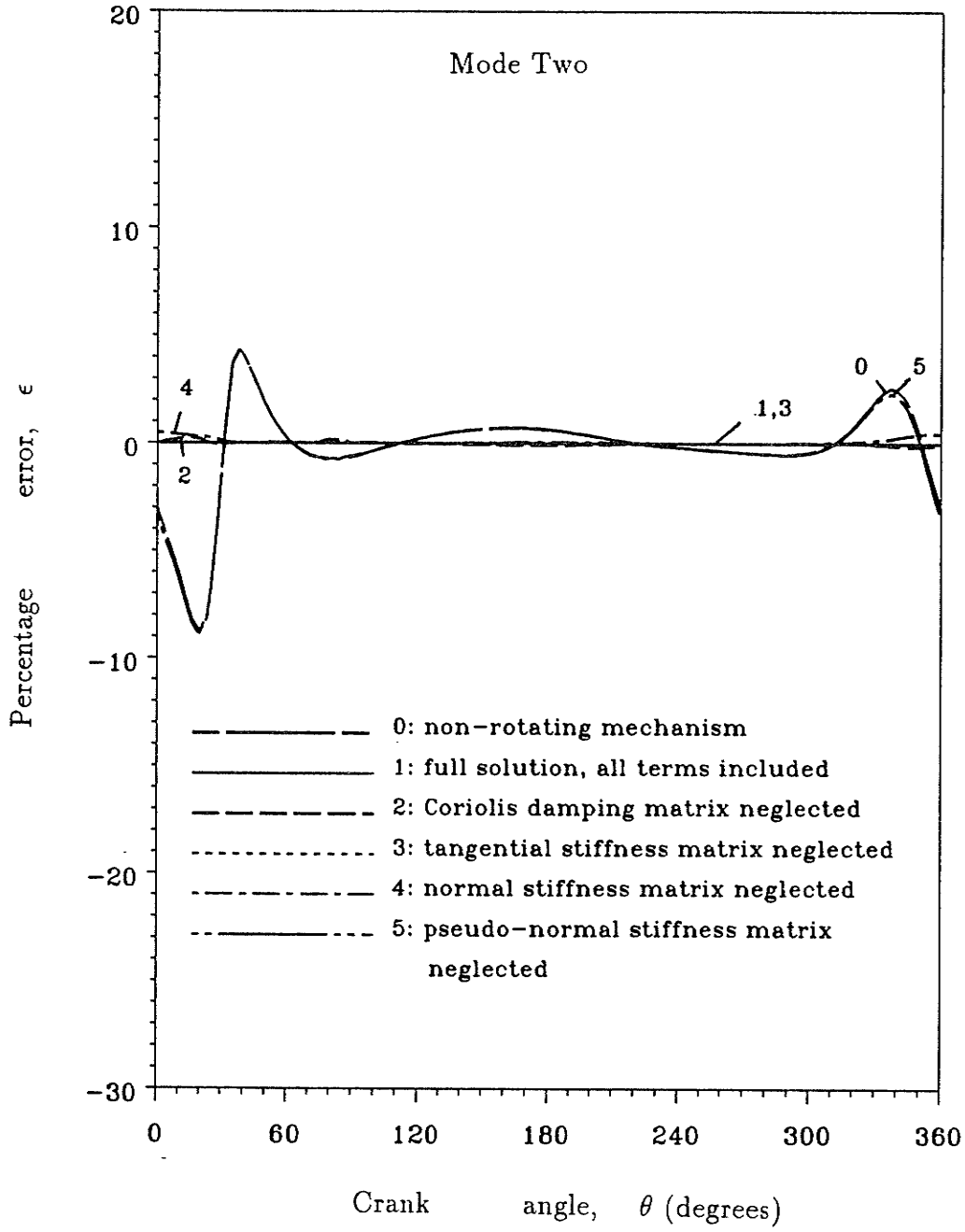

Figure 3.15: Percentage error in natural frequency vs. crank angle, Ω=500 rad/sec

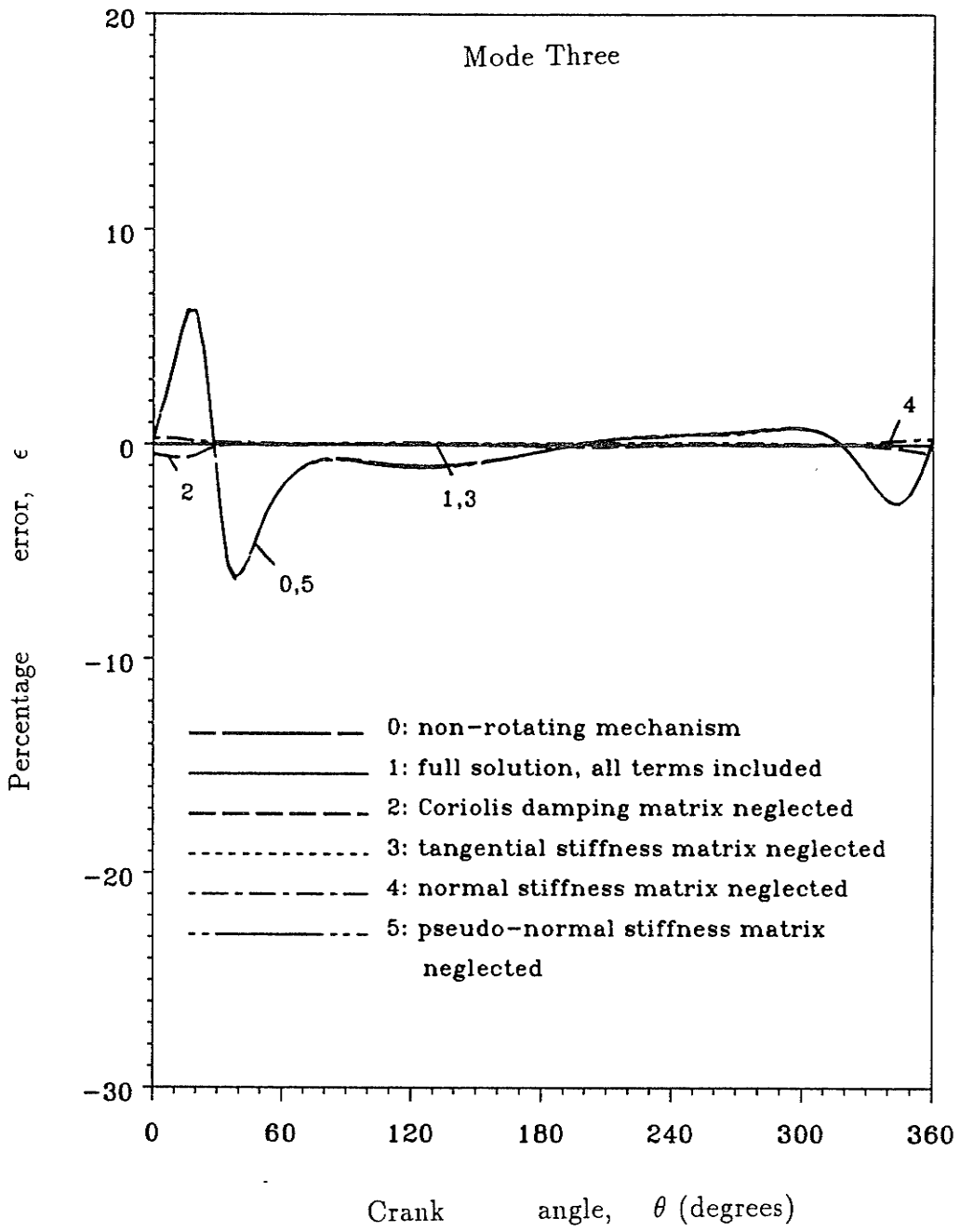

Figure 3.16: Percnetage error in natural frequency vs. crank angle, Ω=500 rad/sec

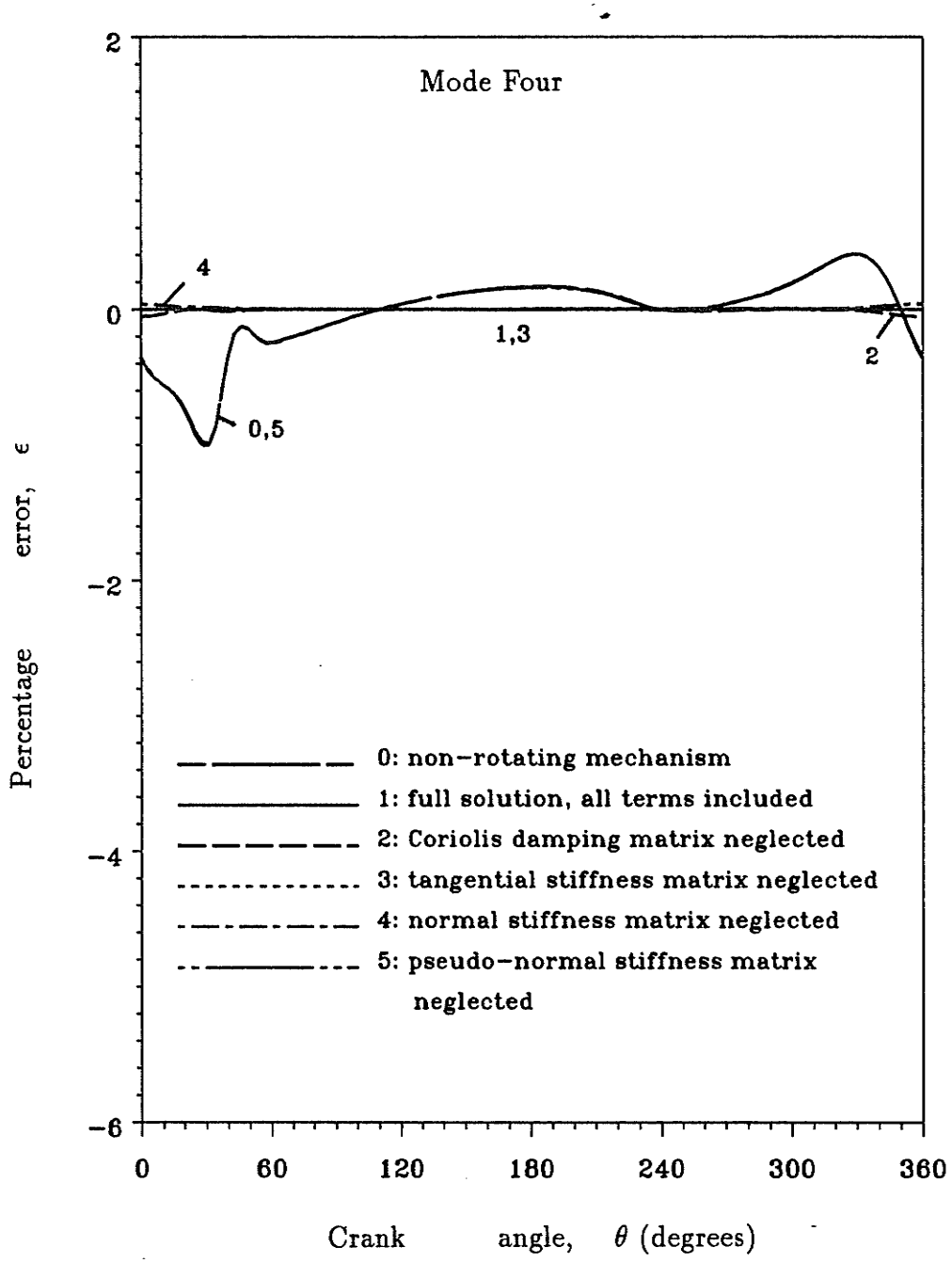

Figure 3.17: Percentage error in natural frequency vs. crank angle, Ω=500 rad/sec

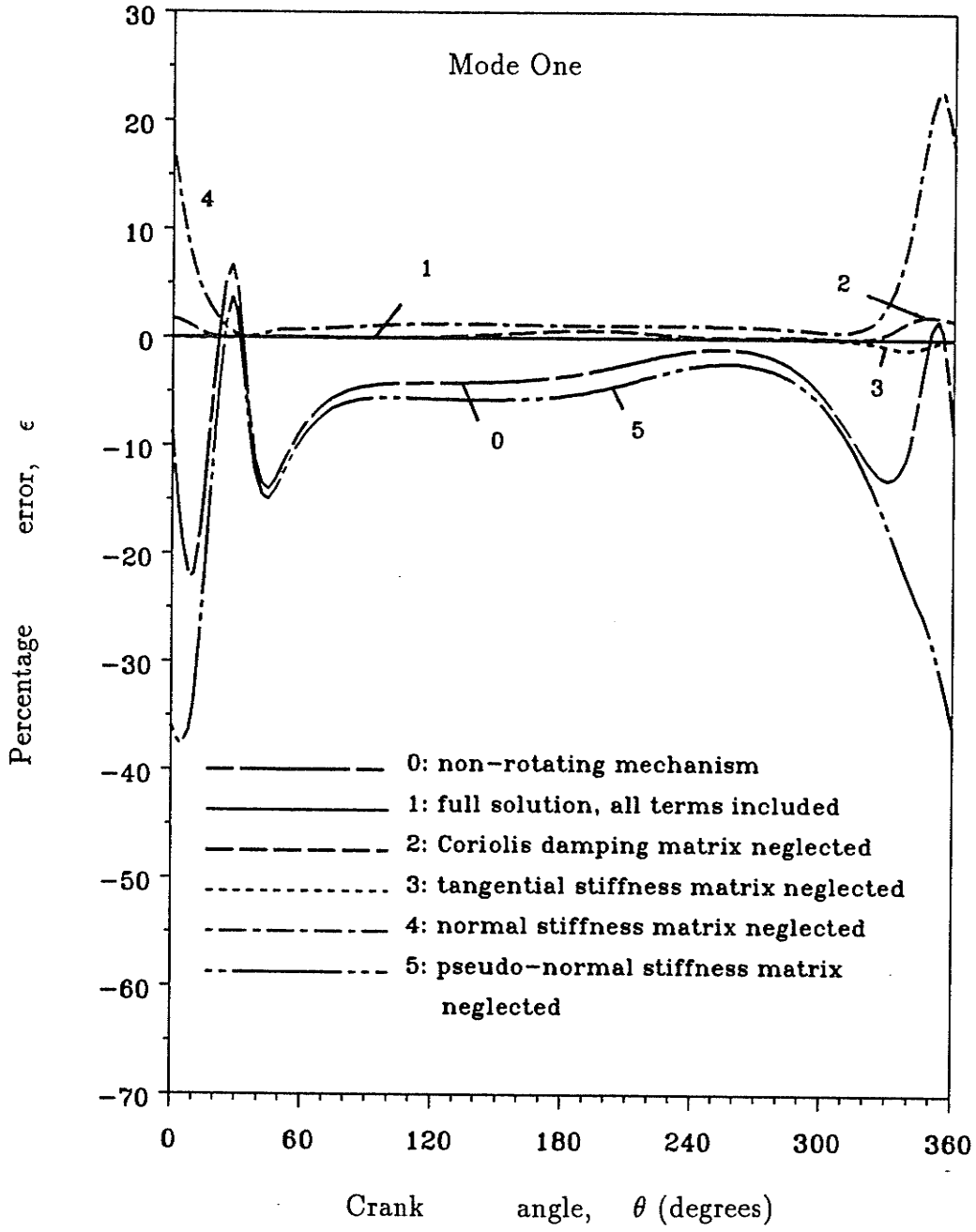

Figure 3.18: Percentage error in natural frequency vs. crank angle, Ω=1000 rad/sec

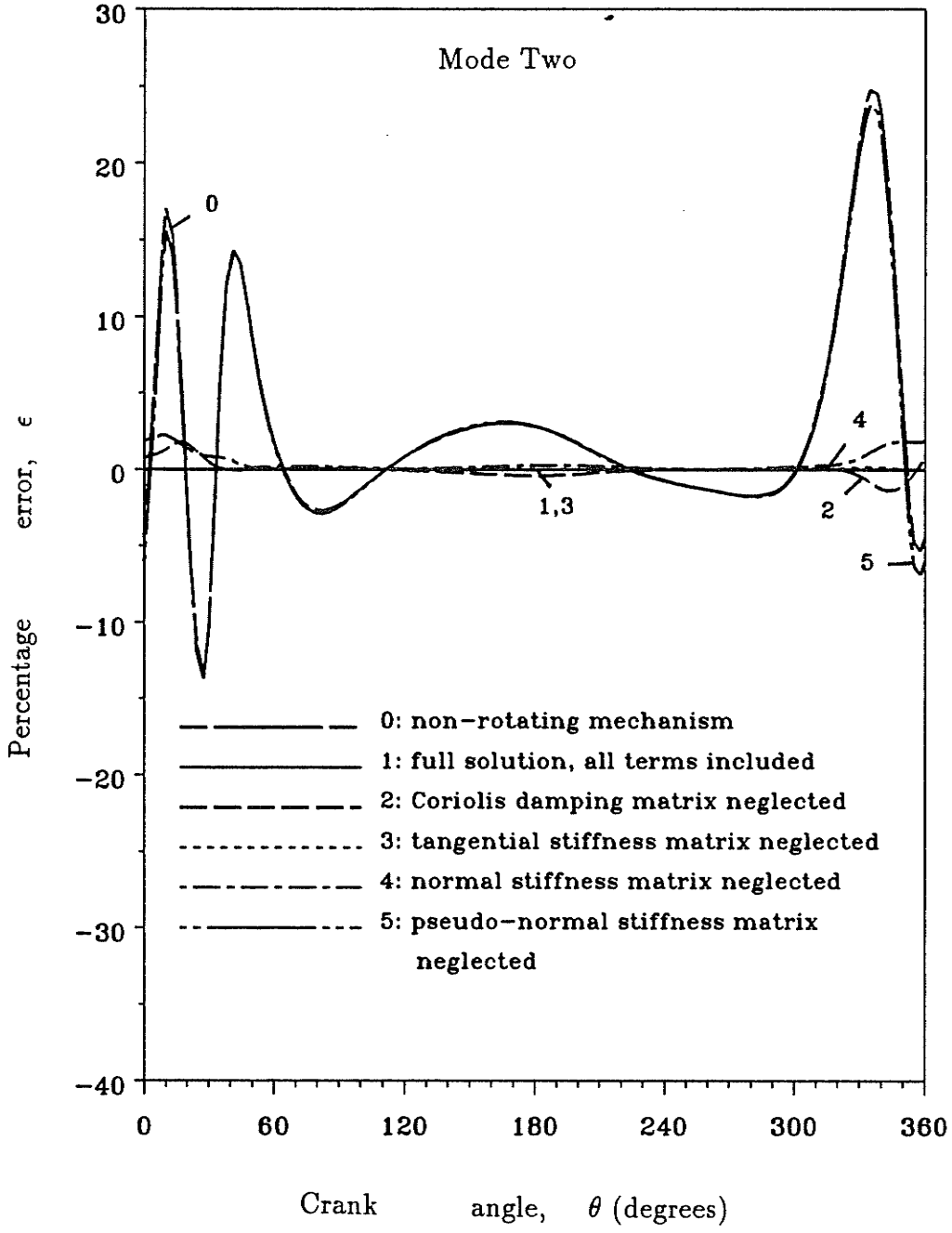

Figure 3.19: Percentage error in natural frequency vs. crank angle, Ω=1000 rad/sec

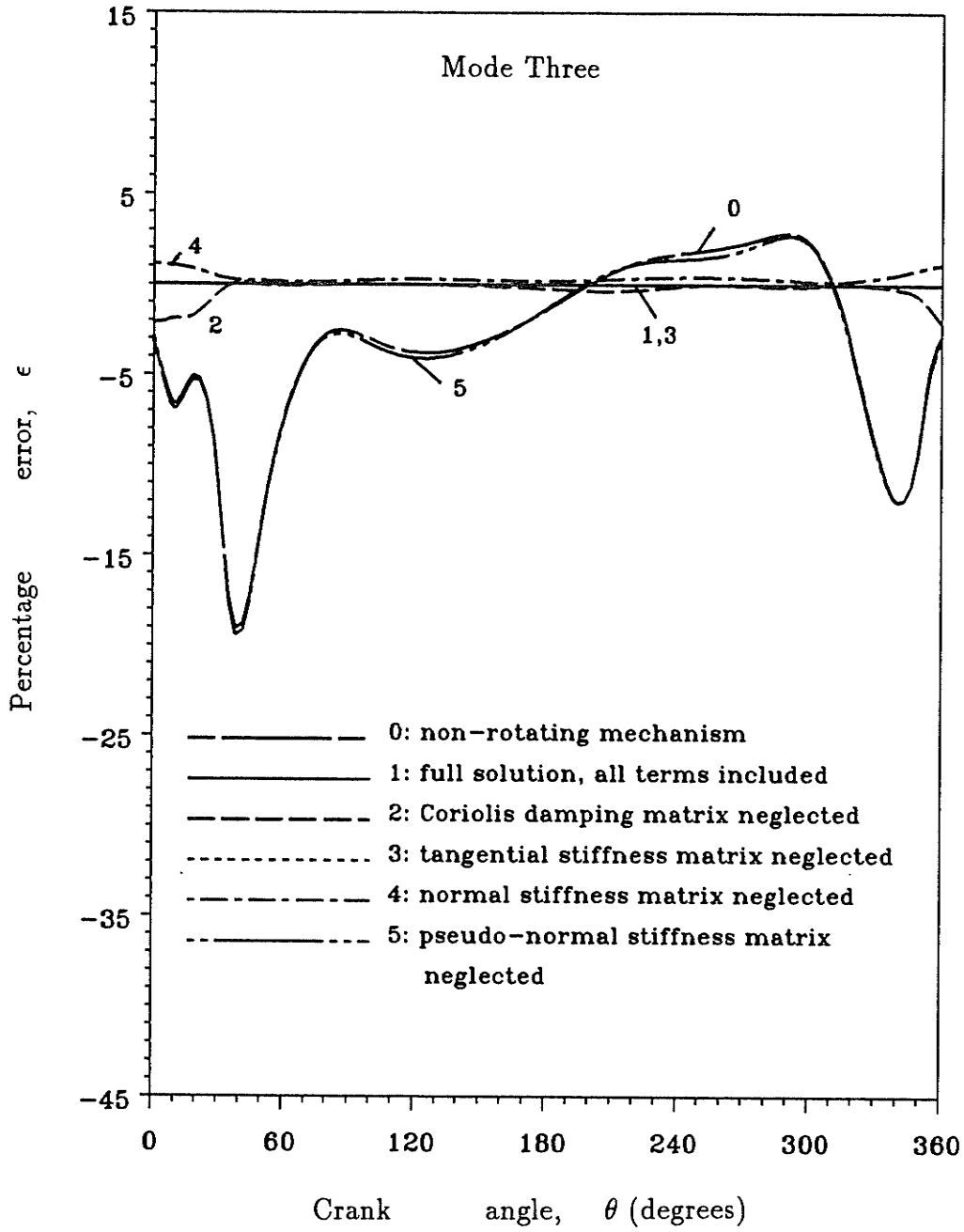

Figure 3.20: Percentage error in natural frequency vs. crank angle, Ω=1000 rad/sec

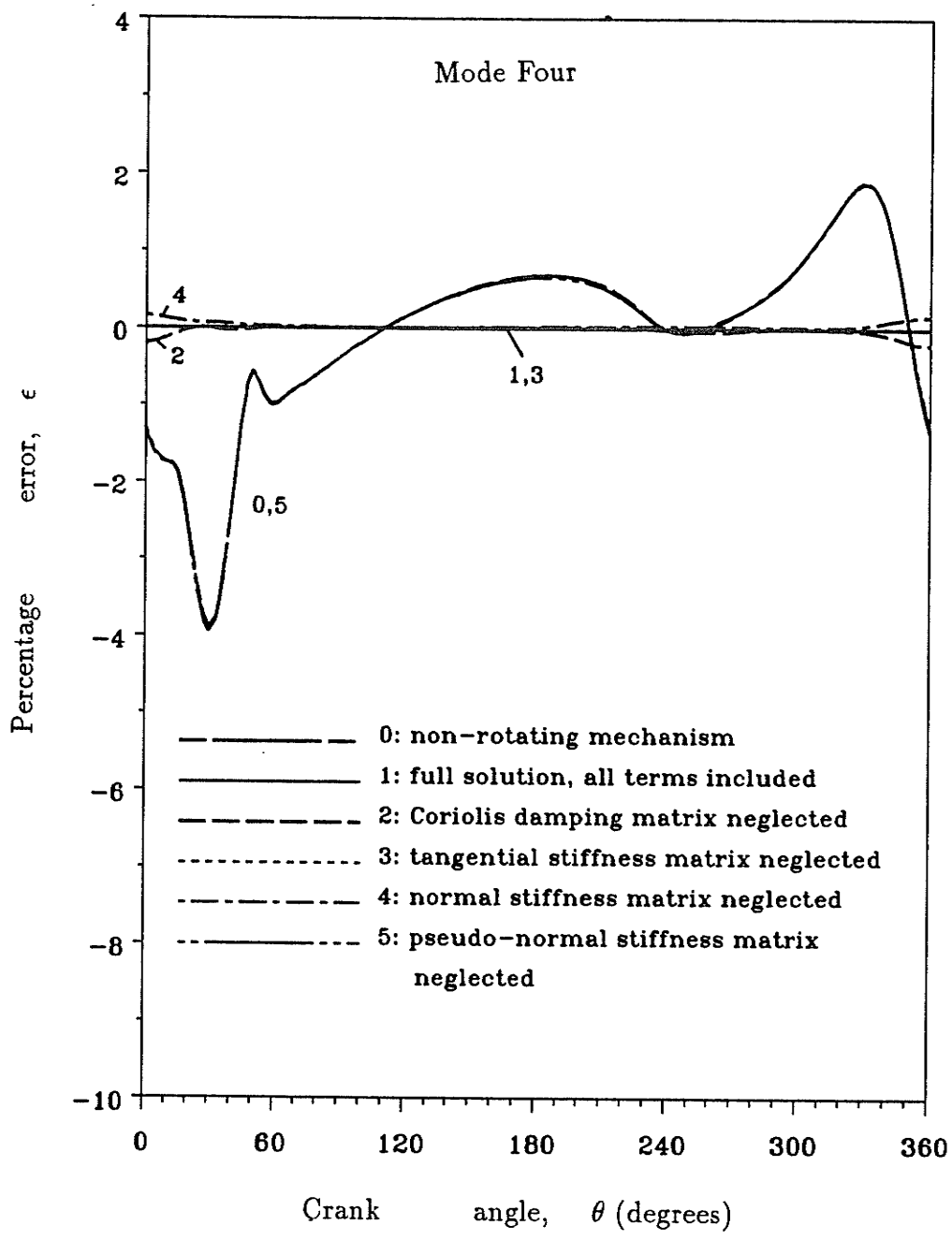

Figure 3.21: Percentage error in natural frequency vs. crank angle, Ω=1000 rad/sec

the predictions from the complete solution. In this way, errors are measured by their departure from $x-$axis. As can be seen from these figures, the neglect of the Coriolis damping matrix and tangential stiffness matrix (cases 2 and 3) over a cycle causes no perceptible errors. However, where there are errors, the errors increase with the increase of speeds as expected, with the largest errors occuring at the begining and ending parts of a cycle. It is apparent that the normal and pseudo-normal stiffness matrices have more pronounced effect on the natural frequency response than any other terms in the equations of motion. Error as high as 38% is experienced at $\Omega = 1000$ rad/sec when the pseudo-normal stiffness term is neglected. It is also observed that the influence of normal stiffness matrix is usually less significant than the pseudo-normal stiffness term.

Finally, the mode shapes for the first four modes are presented in Figures 3.22–3.25, corresponding to $\theta = 10°$ and $\Omega = 1000$ rad/sec. It is noticed that the effects of the extra acceleration terms on the mode shapes are generally small. The only exception to this is the pseudo-normal stiffness term, which has a more significant effect on the mode shapes. Not surprisingly, when the pseudo-normal stiffness term is neglected, the resulting mode shapes are approximately those for a non-rotating mechanism. This is expected in view of the similar trend obtained in the natural frequency results.

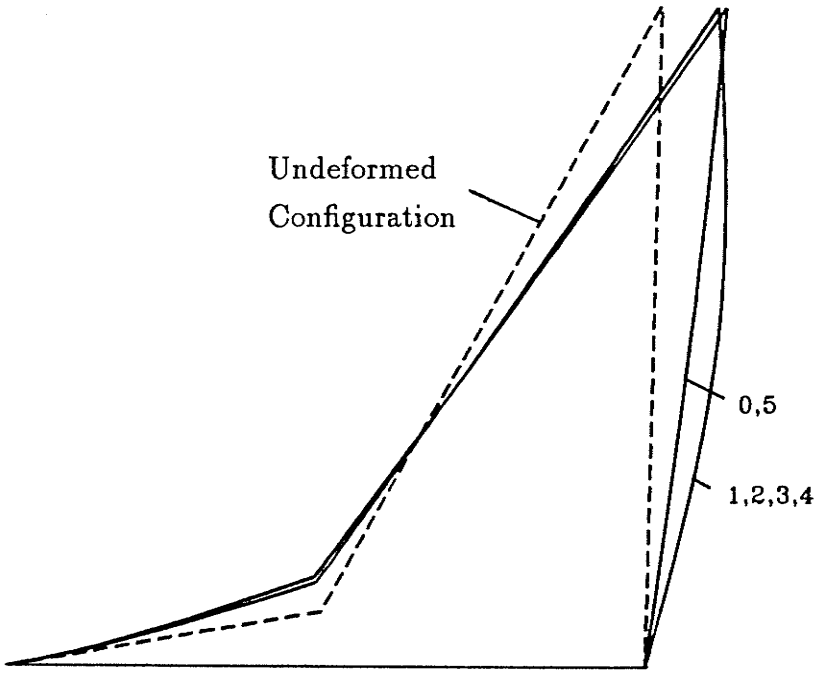

Figure 3.22: Fundamental mode shape,$\theta = 10°, \Omega$=1000 rad/sec

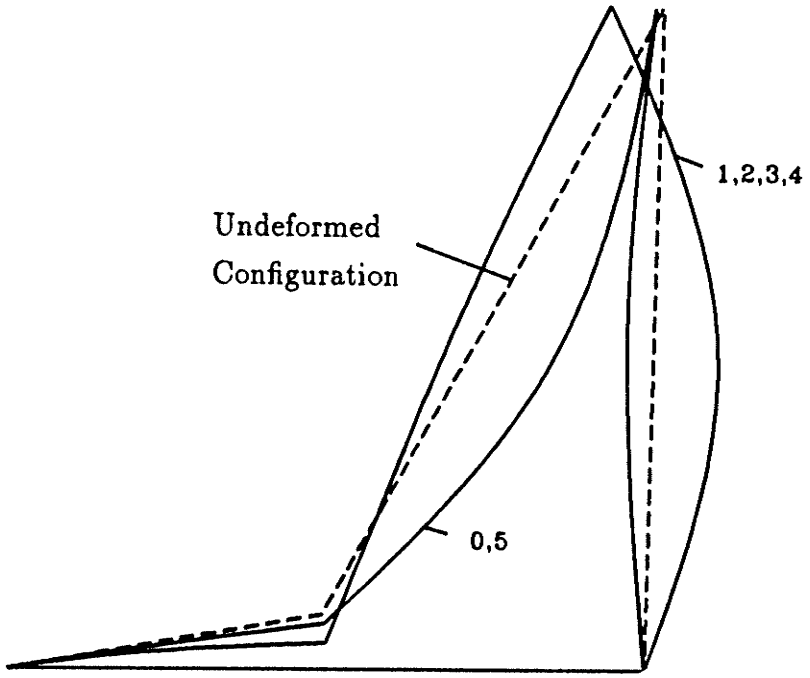

Figure 3.23: Second mode shape, $\theta = 10°, \Omega$=1000 rad/sec

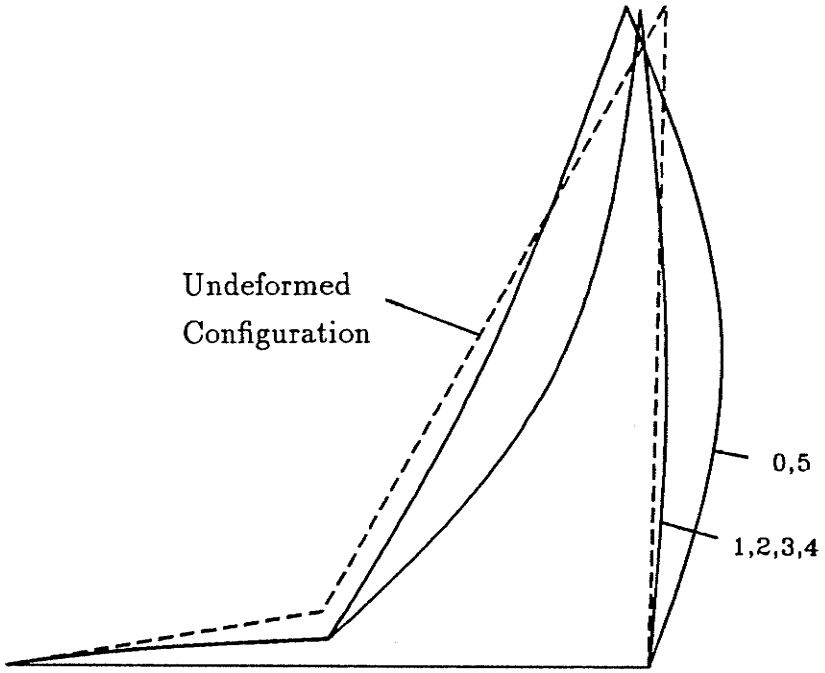

Figure 3.24: Third mode shape, $\theta = 10°, \Omega$=1000 rad/sec

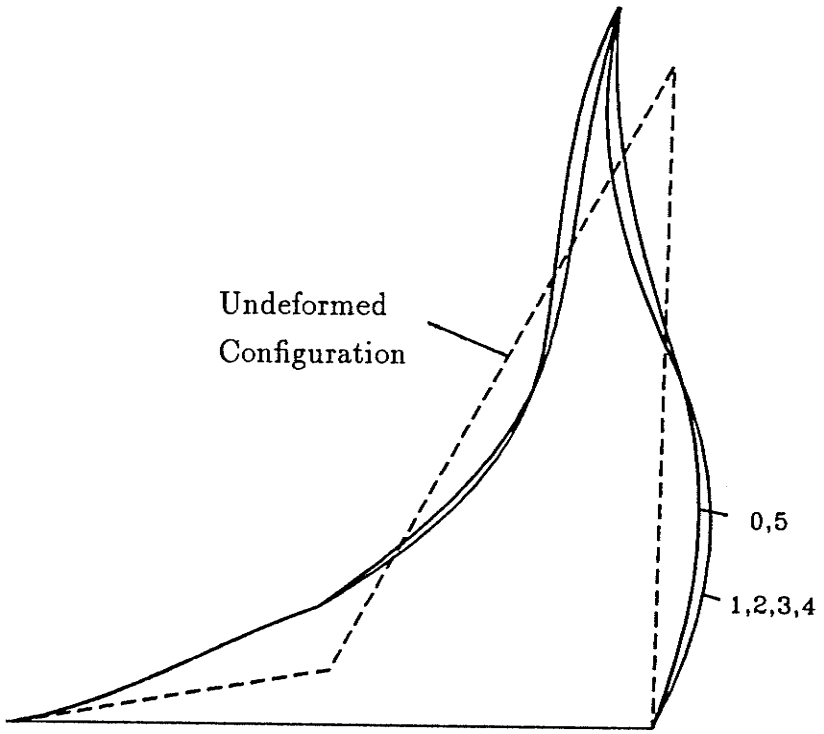

Figure 3.25: Forth mode shape, $\theta = 10°, \Omega$=1000 rad/sec

Chapter 4

Conclusions and Recommendations

4.1 Conclusions

Presented in this thesis is a systematic formulation dealing with the free kineto-elastovibration analysis of high speed flexible mechanism systems. The derivation of the governing equations of motion is accomplished by using the displacement finite element technique, in which the continuously distributed mass system is modeled by a discrete system with finite number degrees of freedom. Euler-Bernoulli beam type elements are employed in this analysis. Both transverse and longitudinal deflections of the elements are considered in the finite element analysis.

To eliminate the singularity in the global matrices, the mechanism is assumed to behave as an instantaneous structure at every instant of its kinematic motion. It is further assumed that the absolute motion of each elas-

tic member is obtained by superimposing the elastic deformations upon the known rigid body motions.

Special attention in formulating the linearized equations of motion was paid to the extra acceleration terms, namely the Coriolis, tangential, normal and pseudo-normal accelerations of elastic deformations. As was illustrated, the inclusion of these terms in the equations of motion leads to complex eigenproblem. A special algorithm was employed to solve the resulting problem. Basically, the solution procedure consists of transforming the n equations of motion into a $2n$ equation system with real coefficient matrices. Then the reduced equations are solved by the QZ algorithm. A finite element program was developed in accordance with the foregoing formulation and solution scheme. With some minor modifications, the program can be extended to the analysis of multi-loop planar mechanisms.

A four-bar linkage was used to investigate the effects of extra acceleration terms on the dynamic characteristics of flexible mechanism systems. The numerical results show that, among these extra acceleration terms, the normal and pseudo-normal stiffness terms have the most significant influence on the natural frequencies. Large errors are experienced when either term is neglected. As expected, it is found that the normal acceleration term has less significant effect on the natural frequencies than the pseudo-normal accelerations. Also, incorrect stability prediction will result when the pseudo-normal

acceleration term is neglected. On the other hand, the effects of the Coriolis and tangential acceleration terms are negligible if neglected in the analysis.

The influence of the extra acceleration terms on the mode shapes is found to be small. The only exception to this is when the pseudo-normal acceleration term is neglected, which in this case yields mode shapes much close to those of a non-rotating mechanism.

In conclusion, the normal and pseudo-normal stiffnesses should be included in the equations of motion, to accurately model the free vibration problem of high speed flexible mechanisms.

4.2 Recommendations

To comprehend the influence of the extra acceleration terms on the dynamics of high speed flexible mechanisms more completely, it is recommended that

- forced kineto-elastovibration analysis, including the determination of the elastic deflections, stresses and strains at any point of a moving member, be carried out considering the extra acceleration terms.
- higher order polynomials be employed to improve the accuracy of numerical predictions.
- Timoshenko beam theory be used when modeling short stubby beams.

Bibliography

[1] Lowen, G. G. and Chassapis, C., The Elastic Behavior of Linkages: An Update, Mechanism and Machine Theory, Vol. 21, 1986, pp. 33-42.

[2] Thompson, B. S. and Sung, C. K., A Survey of Finite Element Techniques for Mechanism Design, Mechanism and Machine Theory, Vol. 21, 1986, pp. 351-359.

[3] Neubauer, A. H. Jr., Cohen, R. and Hall, A. S. Jr., An Analytical Study of the Dynamics of an Elastic Linkage, ASME Journal of Engineering for Industry, Vol. 88, 1966, pp. 311-317.

[4] Viscomi, B. V. and Ayre, R. S., Nonlinear Dynamic Response of Elastic Slider-Crank Mechanism, ASME Journal of Engineering for Industry, Vol. 93, 1971, pp. 251-262.

[5] Chu, S. C. and Pan, K. C., Dynamic Response of a High-Speed Slider Crank Mechanism with an Elastic Connecting Rod, ASME Journal of Engineering for Industry, Vol. 97, 1975, pp. 542-549.

[6] Sutherland, G. H., Analytical and Experimental Investigation of a High-Speed Elastic-Membered Linkage, ASME Journal of Engineering for Industry, Vol. 98, 1976, pp. 788-794.

[7] Kohli, D, Hunter, D. and Sandor, G. N., Elastodynamic Analysis of a Completely Elastic System, ASME Journal of Engineering for Industry, Vol. 99, 1977, pp. 604-609.

[8] Thompson, B. S. and Barr, A. D. S., A Variational Principle for the Elastodynamic Motion of Planar Linkages, ASME Journal of Engineering for Industry, Vol. 98, 1976, pp. 1306-1312.

[9] Thompson, B. S., The Analysis of an Elastic Four-Bar Linkage on a Vibrating Foundation Using a Variational Method, ASME Journal of Mechanical Design, Vol. 102, 1980, pp. 320-328.

[10] Jandrasits, W. G. and Lowen, G. G., The Elastic-Dynamic Behavior of a Counterweighted Rocker Link with an Overhanging Endmass in a Four-Bar Linkage Part I: Theory, ASME Journal of Mechanical Design, Vol. 101, 1979, pp. 77-88.

[11] Sanders, J. R. and Tesar, D., The Analytical and Experimental Evaluation of Vibratory Oscillations in Realistically Proportioned Mechanisms, ASME Journal of Mechanical Design, Vol. 100, 1978, pp. 762-768.

[12] Winfrey, R. C., Elastic Linkage Mechanism Dynamics, ASME Journal of Engineering for Industry, Vol. 93, 1971, pp. 268-272.

[13] Winfrey, R. C., Dynamic Analysis of Elastic Link Mechanisms by Reduction of Coordinates, ASME Journal of Engineering for Industry, Vol. 94, 1972, pp. 577-582.

[14] Erdman, A. G., Sandor, G. N. and Oakberg, R. G., A General Method for Kineto-Elastodynamic Analysis and Synthesis of Mechanisms, ASME Journal of Engineering for Industry, Vol. 94, 1972, pp. 1193-1205.

[15] Bahgat, B. M., and Willmert, K. D., Finite Element Vibrational Analysis of Planar Mechanisms, Mechanism and Machine Theory, Vol. 11, 1976, pp. 47-71.

[16] Cleghorn, W. L., Fenton, R. G. and Tabarrok, B., Finite Element Analysis of High-Speed Flexible Mechanisms, Mechanism and Machine Theory, Vol. 16, 1981, pp. 407-424.

[17] Cleghorn, W. L., Fenton, R. G. and Tabarrok, B., Steady-State Vibrational Response of High-Speed Flexible Mechanisms, Mechanism and Machine Theory, Vol. 19, 1984, pp. 417-423.

[18] Cleghorn, W. L. and Chao, K. C., Kineto-Elastodynamic Modeling of Mechanisms Employing Linearly Tapered Beam Finite Elements, Mechanism and Machine Theory, Vol. 23, 1988, pp. 333-342.

[19] Alexander, R. M. and Lawrence, K. L., An Experimental Investigation of the Dynamic Response of an Elastic Mechanism, ASME Journal of Engineering for Industry, Vol. 96, 1974, pp. 268-274.

[20] Midha, A., Erdman, A. G. and Frohrib, D. A., An Approximate Method for the Dynamic Analysis of Elastic Linkages, ASME Journal of Engineering for Industry, Vol. 99, 1977, pp. 449-455.

[21] Midha, A., Erdman, A. G. and Frohrib, D. A., Finite Element Approach to Mathematical Modeling of High-Speed Elastic Linkages, Mechanism and Machine Theory, Vol. 13, 1978, pp. 603-618.

[22] Midha, A., Erdman, A. G. and Frohrib, D. A., A Closed-Form Numerical Algorithm for the Periodic Response of High-Speed Elastic Linkages, ASME Journal of Mechanical Design, Vol. 101, 1979, pp. 154-162.

[23] Turcic, D. A., A General Approach to the Dynamic Analysis of Elastic Mechanism Systems, Doctoral Dissertation, The Pennsylvania State University, Nov. 1982.

[24] Turcic, D. A. and Midha, A., Generalized Equations of Motion for the Dynamic Analysis of Elastic Mechanism Systems, ASME Journal of Dynamic Systems, Measurements, and Control, Vol. 106, 1984, pp. 243-248.

[25] Turcic, D. A. and Midha, A., Dynamic Analysis of Elastic Mechanism Systems. Part I: Application, ASME Journal of Dynamic Systems, Measurements, and Control, Vol. 106, 1984, pp. 249-254.

[26] Turcic, D. A. and Midha, A., Dynamic Analysis of Elastic Mechanism Systems. Part II: Experimental Results, ASME Journal of Dynamic Systems, Measurements, and Control, Vol. 106, 1984, pp. 255-260.

[27] Nath, P. K. and Ghosh, A., Kineto-Elastodynamic Analysis of Mechanisms by Finite Element Method, Mechanism and Machine Theory, Vol. 15, 1980, pp. 179-197.

[28] Nath, P. K. and Ghosh, A., Steady State Response of Mechanisms with Elastic Links by Finite Element Methods, Mechanism and Machine Theory, Vol. 15, 1980, pp. 199-211.

[29] Thompson, B. S., Variational Formulations for the Finite Element Analysis of Noise Radiation from High-Speed Machinery, ASME Journal of Engineering for Industry, Vol. 103, 1981, pp. 385-391.

[30] Thompson, B. S., A Variational Formulation for the Finite Element Analysis of Vibratory and Acoustical Response of High Speed Machinery, Journal of Sound and Vibration, Vol. 89, 1983, pp. 7-15.

[31] Thompson, B. S. and Sung, C. K., A Variational Formulation for the Nonlinear Finite Element Analysis of Flexible Linkages: Theory, Implementation and Experimental Results, ASME Journal of Mechanisms, Transmissions, and Automation in Design, Vol. 106, 1984, pp. 482-488.

[32] Sung, C. K., Thompson, B. S., Xing, T. M. and Wang, C. H., An Experimental Study on the Nonlinear Elastodynamic Response of Linkage Mechanisms, Mechanism and Machine Theory, Vol. 21, 1986, pp. 121-133.

[33] Sunada, W. and Dubowsky, S., The Application of Finite Element Methods to the Dynamic Analysis of Flexible Spatial and Co-Planar Linkage Systems, ASME Journal of Mechanical Design, Vol. 103, 1982, pp. 643-651.

[34] Sunada, W. H. and Dubowsky, S., On the Dynamic Analysis and Behavior of Industrial Robotic Manipulators with Elastic Members, ASME Journal of Mechanisms, Transmissions, and Automation in Design, Vol. 105, 1983, pp. 42-51.

[35] Bricout, J. N., Debus, J. C. and Micheau, P., A Finite Element Model for the Dynamics of Flexible Manipulators, Mechanism and Machine Theory, Vol. 25, 1990, pp. 119-128.

[36] Zienkiewicz, O. C., Wood, W. L., Hine, N. W. and Taylor, R. L., A Unified Set of Single Step Algorithms, Part 1: General Formulation and Applications, International Journal for Numerical Methods in Engineering, Vol. 20, 1984, pp. 1529-1552.

[37] Wood, W. L., A Unified Set of Single Step Algorithms, Part 2: Theory, International Journal for Numerical Methods in Engineering, Vol. 20, 1984, pp. 2303-2309.

[38] Sadler, J. P. and Sandor, G. N., A Lumped Parameter Approach to Vibration and Stress Analysis of Elastic Linkages, ASME Journal of Engineering for Industry, Vol. 95, 1973, pp. 549-557.

[39] Sadler, J. P. and Sandor, G. N., Nonlinear Vibration Analysis of Elastic Four-Bar Linkages, ASME Journal of Engineering for Industry, Vol. 96, 1974, pp. 411-419.

[40] Sadler, J. P., On the Analytical Lumped-Mass Model of an Elastic Four-Bar Mechanism, ASME Journal of Engineering for Industry, Vol. 97, 1975, pp. 561-565.

[41] Golebiewski, E. P. and Sadler, J. P., Analytical and Experimental Investigation of Elastic Slider-Crank Mechanisms, ASME Journal of Engineering for Industry, Vol. 98, 1976, pp. 1266-1271.

[42] Giovagnoni, M., Simplifications Using Isoparametric Elements in Flexible Linkage Analysis, International Journal for Numerical Methods in Engineering, Vol. 28, 1989, pp. 967-977.

[43] Imam, I., Sandor, G. N. and Kramer, S. N., Deflection and Stress Analysis in High Speed Planar Mechanisms with Elastic Links, ASME Journal of Engineering for Industry, Vol. 95, 1973, pp. 541-548.

[44] Kalaycioglu, S. and Bagci, C., Determination of the Critical Operating Speeds of Planar Mechanisms by the Finite Element Method Using Planar Actual Line Elements and Lumped Mass Systems, ASME Journal of Mechanical Design, Vol. 101, 1979, pp. 210-223.

[45] Han, Ray P. S., Zu, Jean Wu-Zheng and Xu, Z. Y., Kineto-Elastodynamic Analysis of Mechanisms Revisited, submitted to ASME Journal of Mechanisms, Transmissions, and Automation in Design, 1990.

[46] Han, Ray P. S., Xu, Z. Y. and Zu, Jean Wu-Zheng, On the Free Kineto-Elastovibrations of High Speed Mechanisms, submitted to ASME Journal of Mechanisms, Transmissions, and Automation in Design, 1990.

[47] Han, Ray P. S., Xu, Z. Y. and Zu, Jean Wu-Zheng, On the Eigensolutions of Elastic Mechanisms, CSME Mechanical Engineering Forum 1990, Toronto, June 1990.

[48] Hurty, W. C. and Rubinstein, M. F., Dynamics of Structures, Prentice-Hall Inc., 1964.

[49] Moler, C. B. and Stewart, G. W., An Algorithm for Generalized Matrix Eigenvalue Problem, SIAM Journal on Numerical Analysis, Vol. 10, 1973, pp. 241-256.

Appendix A

List of Element Matrices

The conventional mass matrix and the secondary mass matrix are given by Equations (2.10) and (2.11), respectively. Both matrices are listed below.

$$[m_e] = \frac{m}{420}\begin{bmatrix} 140 & 0 & 0 & 70 & 0 & 0 \\ 0 & 156 & 22l & 0 & 54 & -13l \\ 0 & 22l & 4l^2 & 0 & 13l & -3l^2 \\ 70 & 0 & 0 & 140 & 0 & 0 \\ 0 & 54 & 13l & 0 & 156 & -22l \\ 0 & -13l & -3l^2 & 0 & -22l & 4l^2 \end{bmatrix}$$

$$[m_e^*] = \frac{m}{60}\begin{bmatrix} 0 & -21 & -3l & 0 & -9 & 2l \\ 21 & 0 & 0 & 9 & 0 & 0 \\ 3l & 0 & 0 & 2l & 0 & 0 \\ 0 & -9 & -2l & 0 & -21 & 3l \\ 9 & 0 & 0 & 21 & 0 & 0 \\ -2l & 0 & 0 & -3l & 0 & 0 \end{bmatrix}$$

The explicit expression for the structural stiffness matrix, given by Equa-

tion (2.22), is as follows

$$[k_e^s] = \begin{bmatrix} EA/l & 0 & 0 & -EA/l & 0 & 0 \\ 0 & 12EI/l^3 & 6EI/l^2 & 0 & -12EI/l^3 & 6EI/l^2 \\ 0 & 6EI/l^2 & 4EI/l & 0 & -6EI/l^2 & 2EI/l \\ -EA/l & 0 & 0 & EA/l & 0 & 0 \\ 0 & -12EI/l^3 & -6EI/l^2 & 0 & 12EI/l^3 & -6EI/l^2 \\ 0 & 6EI/l^2 & 2EI/l & 0 & -6EI/l^2 & 4EI/l \end{bmatrix}$$

The three component matrices of the pseudo-normal stiffness matrix, defined by Equation (2.26), are given below,

$$[k_e^{f1}] = \frac{F_r}{30l} \begin{bmatrix} 0 & 0 & 0 & 0 & 0 & 0 \\ 0 & 36 & 3l & 0 & -36 & 3l \\ 0 & 3l & 4l^2 & 0 & -3l & -l^2 \\ 0 & 0 & 0 & 0 & 0 & 0 \\ 0 & -36 & -3l & 0 & 36 & -3l \\ 0 & 3l & -l^2 & 0 & -3l & 4l^2 \end{bmatrix}$$

$$[k_e^{f2}] = \frac{\rho A a_l}{60} \begin{bmatrix} 0 & 0 & 0 & 0 & 0 & 0 \\ 0 & -36 & 0 & 0 & 36 & -6l \\ 0 & 0 & -6l^2 & 0 & 0 & l^2 \\ 0 & 0 & 0 & 0 & 0 & 0 \\ 0 & 36 & 0 & 0 & -36 & 6l \\ 0 & -6l & l^2 & 0 & 6l & -2l^2 \end{bmatrix}$$

$$[k_e^{f3}] = \frac{\rho A l \dot{\theta}^2}{420} \begin{bmatrix} 0 & 0 & 0 & 0 & 0 & 0 \\ 0 & 180 & 6l & 0 & -180 & 27l \\ 0 & 6l & 24l^2 & 0 & -6l & -4l^2 \\ 0 & 0 & 0 & 0 & 0 & 0 \\ 0 & -180 & -6l & 0 & 180 & -27l \\ 0 & 27l & -4l^2 & 0 & -27l & 10l^2 \end{bmatrix}$$

where the notations are the same as those defined in chapter 2.

Appendix B

User's Manual for Program FKEV

Input parameters:

NGN	number of geometric nodes
NE	number of elements
NEI(3)	number of elements for each moving member
N12(10,2)	the end node numbers of the NE elements
NBC(2)	the number of the constrained nodes
NDOF(2,3)	information for boundary conditions
A(3)	cross sectional area of the moving links
E(3)	modulus of elasticity of the moving links
AI(3)	area moment of inertia of the moving links
RHO(3)	mass density of the moving links
RL(4)	length of the four links
NW	number of different angular velocities

	interested in the analysis
WN(10)	input angular velocities
DDTH(1)	input angular acceleration
DELT	angle increment
INDEX	motion index, referring to Table 3.3
MKC	print control variable

Output parameters:

ANGLE	crank angle
P1(73,10)	fundamental mode frequency
P2(73,10)	second mode frequency
P3(73,10)	third mode frequency
P4(73,10)	forth mode frequency

Function of the subroutines:

subroutine MKQ	forming the system matrices and solving for the natural frequencies and corresponding mode shapes
subroutine MKQE	forming the element matrices
subroutine RBK	rigid body kinematics of the mechanism
subroutine REF	determining the right hand end forces of the NE elements.

Appendix C

Program for Free Kineto-Elastovibration Analysis

```
                        PROGRAM FKEV

CCCCCCCCCCCCCCCCCCCCCCCCCCCCCCCCCCCCCCCCCCCCCCCCCCCCCCCCCCCCCCCCCCCCCCCCCCCCCCC
C                                                                              C
C       This is to do Free Kineto-ElastoVibration analysis of                  C
C              a four-bar crank rocker mechhanism                              C
C                                                                              C
CCCCCCCCCCCCCCCCCCCCCCCCCCCCCCCCCCCCCCCCCCCCCCCCCCCCCCCCCCCCCCCCCCCCCCCCCCCCCCC

      IMPLICIT REAL*8(A-H,O-Z)
      COMMON /MKQ1/NGN,NE,NBC(2),NEI(3),N12(10,2),NDOF(2,3)
      COMMON /MKQ2/RL(4),RHOA(3),TH(3),DTH(3),DDTH(3),EA(3),EI(3),
     1 ALX(20),FR(20),TR,DELT
      COMMON /SWITCH/INDEX,MKC
      COMMON /PLOT/P1(73,10),P2(73,10),P3(73,10),P4(73,10),P5(73,10)
      DIMENSION RHO(3),A(3),E(3),AI(3),DDU0(50),WN(10)
      DIMENSION AA(60,60),BB(60,60),WK(7200),RZ(7200),BET(60),RALF(120)
      COMPLEX Z(60,60),ALF(60)
      TR=DATAN(1.D0)/45.
      READ(5,*) NGN,NE,(NEI(I),I=1,3),INDEX,MKC
      DO 10 I=1,NE
```

```
10 READ(5,*) N12(I,1),N12(I,2)
   DO 20 I=1,2
20 READ(5,*) NBC(I), (NDOF(I,J),J=1,3)
   READ(5,*) (RL(I),I=1,4)
   DO 30 I=1,3
   READ(5,*) RHO(I),A(I),E(I),AI(I)
   RHOA(I)=RHO(I)*A(I)
   EA(I)=E(I)*A(I)
30 EI(I)=E(I)*AI(I)
   READ(5,*) DDTH(1),DELT
   READ(5,*) NW,(WN(I),I=1,NW)
   ND=IDINT(360.0/DELT+1.5)
   WRITE(6,200) NGN,NE,(NEI(I),I=1,3)
   NGN=3*NGN
   NN=NGN+2
   NNO=0
   DO 3 I=1,2
   DO 3 J=1,3
 3 NNO=NNO+NDOF(I,J)
   NNNO=NN-NNO
   N=2*NNNO
   N1=2*N*N
   N2=2*N
   WRITE(6,225)
   DO 40 I=1,NE
40 WRITE(6,230) I,N12(I,1),N12(I,2)
   WRITE(6,245)
   DO 50 I=1,2
50 WRITE(6,230) NBC(I), (NDOF(I,J),J=1,3)
   WRITE(6,260) (RL(I),I=1,4)
   DO 100 IW=1,NW
   DTH(1)=WN(IW)
   WRITE(6,270) DTH(1),DDTH(1),DELT
   DO 90 ITH=1,ND
   TH(1)=(ITH-1)*DELT*TR
   CALL RBK(DDUO)
   CALL REF
   CALL MKQ(N,N1,N2,NN,ITH,DDUO,AA,BB,WK,BET,RZ,RALF,ALF,Z,IW)
90 CONTINUE
```

```
100 CONTINUE
    DO 110 ITH=1,ND
    ANGLE=(ITH-1)*DELT
    WRITE(1,400) ANGLE,(P1(ITH,IW),IW=1,NW)
    WRITE(2,400) ANGLE,(P2(ITH,IW),IW=1,NW)
    WRITE(3,400) ANGLE,(P3(ITH,IW),IW=1,NW)
110 WRITE(4,400) ANGLE,(P4(ITH,IW),IW=1,NW)
200 FORMAT(/1X,'INPUT DATA'//
   1 10X,'NGN=',I2,5X,'NE=',I2,5X,'N1=',I2,5X,'N2=',I2,5X,
   2 'N3=',I2/)
225 FORMAT(10X,'NUMBER OF ELEMENTS AND CORRESPONDING END NODES'/)
230 FORMAT(10X,4I8)
245 FORMAT(/10X,'THE BOUNDARY CONDITIONS'/)
260 FORMAT(/10X,'THE LENGTHS OF THE FOUR BARS:'//10X,4F8.2)
270 FORMAT(/10X,'THE VELOCITY AND ACCELERATION OF THE INPUT LINK'//
   1 10X,'W1=',F7.2,5X,'E1=',F7.2,5X,'DELT=',F7.2//)
400 FORMAT(F5.0,6F14.5)
    STOP
    END

    SUBROUTINE MKQ(N,N1,N2,NN,ITH,DDUO,AA,BB,WK,B,RZ,RA,A,Z,IW)

    IMPLICIT REAL*8(A-H,O-Z)
    COMMON /MKQ1/NGN,NE,NBC(2),NEI(3),N12(10,2),NDOF(2,3)
    COMMON /MKQ2/RL(4),RHOA(3),TH(3),DTH(3),DDTH(3),EA(3),EI(3),
   1 ALX(20),FR(20),TR,DELT
    COMMON /SWITCH/INDEX,MKC
    COMMON /PLOT/P1(73,10),P2(73,10),P3(73,10),P4(73,10),P5(73,10)
    DIMENSION NOLD(6),NROW(6),EM(6,6),EC(6,6),EK(6,6),AO(50),
   1 DDUO(50),SM(50,50),SC(50,50),SK(50,50),FREQ(5)
    DIMENSION AA(N,N),BB(N,N),WK(N1),RZ(N1),B(N),RA(N2)
    COMPLEX A(N),Z(N,N),ZO
    DPI=360.*TR
    NNNO=N/2
    DO 1 I=1,NN
    DO 1 J=1,NN
    SM(I,J)=0.
    SK(I,J)=0.
  1 SC(I,J)=0.
```

```
      DO 3 I=1,N
      DO 3 J=1,N
      AA(I,J)=0.
    3 BB(I,J)=0.
      NOLD(1)=3*NBC(1)-2
      NOLD(2)=NOLD(1)+1
      NOLD(3)=NOLD(2)+1
      NOLD(4)=3*NBC(2)-2
      NOLD(5)=NOLD(4)+1
      NOLD(6)=NOLD(5)+1
      DO 10 J=1,3
      IF(NDOF(1,J).EQ.0) NOLD(J)=0
      IF(NDOF(2,J).EQ.0) NOLD(3+J)=0
   10 CONTINUE
      DO 5 IK=1,3,2
      IF(IK-2) 11,11,13
   11 NEO=1
      NE1=NEI(1)
      NESUM=0
      GOTO 14
   13 NEO=NEI(1)+NEI(2)+1
      NE1=NE
      NESUM=NEO-1
   14 DO 5 IE=NEO,NE1
      NESUM=NESUM+1
      N13=N12(IE,1)*3
      N23=N12(IE,2)*3
      CALL MKQE(EM,EK,EC,IK,NESUM)
   15 DO 5 I=1,3
      DO 5 J=1,3
      I1=N13+I-3
      I2=N23+I-3
      J1=N13+J-3
      J2=N23+J-3
      SM(I1,J1)=SM(I1,J1)+EM(I,J)
      SM(I1,J2)=SM(I1,J2)+EM(I,J+3)
      SM(I2,J1)=SM(I2,J1)+EM(I+3,J)
      SM(I2,J2)=SM(I2,J2)+EM(I+3,J+3)
      SK(I1,J1)=SK(I1,J1)+EK(I,J)
```

```
      SK(I1,J2)=SK(I1,J2)+EK(I,J+3)
      SK(I2,J1)=SK(I2,J1)+EK(I+3,J)
      SK(I2,J2)=SK(I2,J2)+EK(I+3,J+3)
      SC(I1,J1)=SC(I1,J1)+EC(I,J)
      SC(I1,J2)=SC(I1,J2)+EC(I,J+3)
      SC(I2,J1)=SC(I2,J1)+EC(I+3,J)
      SC(I2,J2)=SC(I2,J2)+EC(I+3,J+3)
    5 CONTINUE
      KK=0
      NESUM=NEI(1)
      DO 40 IE=NEI(1)+1,NEI(1)+NEI(2)
      KK=KK+1
      NESUM=NESUM+1
      N13=N12(IE,1)*3
      N23=N12(IE,2)*3
      NROW(1)=N13-2
      NROW(2)=N13-1
      NROW(3)=N13
      IF(KK.EQ.1) NROW(3)=NGN+1
      NROW(4)=N23-2
      NROW(5)=N23-1
      NROW(6)=N23
      IF(KK.EQ.NEI(2)) NROW(6)=NN
      CALL MKQE(EM,EK,EC,2, NESUM)
   25 DO 20 I=1,2
      DO 20 J=1,2
      I1=N13+I-3
      I2=N23+I-3
      J1=N13+J-3
      J2=N23+J-3
      SM(I1,J1)=SM(I1,J1)+EM(I,J)
      SM(I1,J2)=SM(I1,J2)+EM(I,J+3)
      SM(I2,J1)=SM(I2,J1)+EM(I+3,J)
      SM(I2,J2)=SM(I2,J2)+EM(I+3,J+3)
      SK(I1,J1)=SK(I1,J1)+EK(I,J)
      SK(I1,J2)=SK(I1,J2)+EK(I,J+3)
      SK(I2,J1)=SK(I2,J1)+EK(I+3,J)
      SK(I2,J2)=SK(I2,J2)+EK(I+3,J+3)
      SC(I1,J1)=SC(I1,J1)+EC(I,J)
```

```
      SC(I1,J2)=SC(I1,J2)+EC(I,J+3)
      SC(I2,J1)=SC(I2,J1)+EC(I+3,J)
      SC(I2,J2)=SC(I2,J2)+EC(I+3,J+3)
   20 CONTINUE
      DO 30 J=1,6
      SM(NROW(3),NROW(J))=SM(NROW(3),NROW(J))+EM(3,J)
      SM(NROW(6),NROW(J))=SM(NROW(6),NROW(J))+EM(6,J)
      SK(NROW(3),NROW(J))=SK(NROW(3),NROW(J))+EK(3,J)
      SK(NROW(6),NROW(J))=SK(NROW(6),NROW(J))+EK(6,J)
      SC(NROW(3),NROW(J))=SC(NROW(3),NROW(J))+EC(3,J)
      SC(NROW(6),NROW(J))=SC(NROW(6),NROW(J))+EC(6,J)
   30 CONTINUE
      DO 35 I=1,2
      DO 35 J=3,6,3
      SM(NROW(I),NROW(J))=SM(NROW(I),NROW(J))+EM(I,J)
      SM(NROW(I+3),NROW(J))=SM(NROW(I+3),NROW(J))+EM(I+3,J)
      SK(NROW(I),NROW(J))=SK(NROW(I),NROW(J))+EK(I,J)
      SK(NROW(I+3),NROW(J))=SK(NROW(I+3),NROW(J))+EK(I+3,J)
      SC(NROW(I),NROW(J))=SC(NROW(I),NROW(J))+EC(I,J)
      SC(NROW(I+3),NROW(J))=SC(NROW(I+3),NROW(J))+EC(I+3,J)
   35 CONTINUE
   40 CONTINUE
      INEW=0
      DO 70 I=1,NN
      DO 45 K=1,6
      IF(I.EQ.NOLD(K)) GOTO 70
   45 CONTINUE
      INEW=INEW+1
      JNEW=0
      DO 60 J=1,NN
      DO 50 K=1,6
      IF(J.EQ.NOLD(K)) GOTO 60
   50 CONTINUE
      JNEW=JNEW+1
      SM(INEW,JNEW)=SM(I,J)
      SK(INEW,JNEW)=SK(I,J)
      SC(INEW,JNEW)=SC(I,J)
   60 CONTINUE
      DDUO(INEW)=DDUO(I)
```

```
 70 CONTINUE
    CALL MAT(NNNO,AO,SMO,DDUO,0)
    DO 22 I=1,NNNO
 22 DDUO(I)=-AO(I)
    IF(MKC.EQ.0) GOTO 150
    WRITE(6,205)
    DO 80 I=1,NNNO
 80 WRITE(6,210) (SM(I,J),J=1,NNNO)
    WRITE(6,215)
    DO 90 I=1,NNNO
 90 WRITE(6,210) (SK(I,J),J=1,NNNO)
    WRITE(6,227)
    DO 100 I=1,NNNO
100 WRITE(6,210) (SC(I,J),J=1,NNNO)
150 CONTINUE
    IA=N
    IB=N
    IZ=N
    IJOB=2
    ZO=DCMPLX(1.DO,0.DO)
    DO 160 I=1,NNNO
    DO 160 J=1,NNNO
    I1=I+NNNO
    J1=J+NNNO
    AA(I1,J)= SM(I,J)
    AA(I,J1)=-SM(I,J)
    AA(I1,J1)=SC(I,J)
    BB(I,J)=SM(I,J)
160 BB(I1,J1)=SK(I,J)
    CALL EIGZF(AA,IA,BB,IB,N,IJOB,RA,B,RZ,IZ,WK,IER)
    IN=1
    DO 180 J=1,N
    DO 180 I=1,N
    Z(I,J)=DCMPLX(RZ(IN),RZ(IN+1))
180 IN=IN+2
    DO 185 I=1,N
    WRITE(6,270) (Z(I,J),J=1,10,2)
185 CONTINUE
    K=0
```

```
      DO 190 I=1,N,2
      K=K+1
      IF(K.GT.5) GOTO 195
      A(I)=DCMPLX(RA(2*I-1)/B(I),RA(2*I)/B(I))
      A(I)=-ZO/A(I)
      FREQ(K)=AIMAG(A(I))/DPI
  190 CONTINUE
  195 CONTINUE
      P1(ITH,IW)=FREQ(1)
      P2(ITH,IW)=FREQ(2)
      P3(ITH,IW)=FREQ(3)
      P4(ITH,IW)=FREQ(4)
      ANGLE=(ITH-1)*DELT
      WRITE(6,182) ANGLE,(FREQ(I),I=1,5)
  182 FORMAT(1X,F5.0,5F12.6)
  205 FORMAT(/10X,'THE MASS MATRIX:'/)
  210 FORMAT(1X,9E14.4)
  215 FORMAT(/10X,'THE STIFFNESS MATRIX:'/)
  227 FORMAT(/10X,'THE EFFECTIVE DAMPING MATRIX:'/)
  270 FORMAT(1X,10E12.4)
      RETURN
      END

      SUBROUTINE MKQE(EM,EK,EC,IBAR,NESUM)

      IMPLICIT REAL*8(A-H,O-Z)
      COMMON /MKQ1/NGN,NE,NBC(2),NEI(3),N12(10,2),NDOF(2,3)
      COMMON /MKQ2/RL(4),RHOA(3),TH(3),DTH(3),DDTH(3),EA(3),EI(3),
     1 ALX(20),FR(20),TR,DELT
      COMMON /SWITCH/INDEX,MKC
      DIMENSION EM(6,6),EK(6,6),EC(6,6),R(6,6),A(6,6),EKG(6,6)
      S1=DSIN(TH(IBAR))
      C1=DCOS(TH(IBAR))
      W2=2.*DTH(IBAR)
      W22=DTH(IBAR)*DTH(IBAR)
      NB=NEI(IBAR)
      EL=RL(IBAR)/FLOAT(NB)
      EL2=EL*EL
      EL3=EL2*EL
```

```
      RHOAEL=RHOA(IBAR)*EL
      DO 10 I=1,6
      DO 10 J=1,6
      EM(I,J)=0.
      EK(I,J)=0.
      EC(I,J)=0.
      EKG(I,J)=0.0
   10 R(I,J)=0.
      R(1,1)=C1
      R(1,2)=S1
      R(2,1)=-S1
      R(2,2)= C1
      R(3,3)=1.
      R(4,4)=C1
      R(4,5)=S1
      R(5,4)=-S1
      R(5,5)= C1
      R(6,6)=1.
      EM(1,1)=RHOAEL/3.
      EM(1,4)=.5*EM(1,1)
      EM(2,2)=13./35.*RHOAEL
      EM(2,3)=11.*EL/210.*RHOAEL
      EM(2,5)=9./70.*RHOAEL
      EM(2,6)=-13.*EL/420.*RHOAEL
      EM(3,3)=EL2*RHOAEL/105.
      EM(3,5)=-EM(2,6)
      EM(3,6)=-EL2*RHOAEL/140.
      EM(4,4)=EM(1,1)
      EM(5,5)=EM(2,2)
      EM(5,6)=-EM(2,3)
      EM(6,6)=EM(3,3)
      EK(1,1)=EA(IBAR)/EL
      EK(1,4)=-EK(1,1)
      EK(2,2)=12.*EI(IBAR)/EL3
      EK(2,3)=6.*EI(IBAR)/EL2
      EK(2,5)=-EK(2,2)
      EK(2,6)=EK(2,3)
      EK(3,3)=4.*EI(IBAR)/EL
      EK(3,5)=-EK(2,6)
```

```
      EK(3,6)=0.5*EK(3,3)
      EK(4,4)=EK(1,1)
      EK(5,5)=EK(2,2)
      EK(5,6)=-EK(2,3)
      EK(6,6)=EK(3,3)
      A3=-0.5*RHOAEL*W22
      A2=RHOAEL*ALX(NESUM)/EL
      A1=-A2-A3+FR(NESUM)/EL
      EKG(2,2)=1.2*A1+0.6*A2+12./35.*A3
      EKG(2,3)= EL*(0.1*(A1+A2)+A3/14.)
      EKG(2,5)=-EKG(2,2)
      EKG(2,6)= EL*(0.1*A1-A3/35.)
      EKG(3,3)=EL2*(2./15.*A1+A2/30.+2./105.*A3)
      EKG(3,5)=-EKG(2,3)
      EKG(3,6)=-EL2*((2.*A1+A2)/60.+A3/70.)
      EKG(5,5)=EKG(2,2)
      EKG(5,6)= EL*(-.1*A1+A3/35.)
      EKG(6,6)=EL2*(2./15.*A1+0.1*A2+3./35.*A3)
      DO 20 I=2,6
      DO 20 J=1,I-1
      EM(I,J)=EM(J,I)
      EK(I,J)=EK(J,I)
      EKG(I,J)=EKG(J,I)
   20 CONTINUE
   22 IF(INDEX.EQ.0) GOTO 40
   31 EC(1,2)=-7.*RHOAEL/20.
      EC(1,3)=-RHOAEL*EL/20.
      EC(1,5)=-3.*RHOAEL/20.
      EC(1,6)= RHOAEL*EL/30.
      EC(2,4)=-EC(1,5)
      EC(3,4)= EC(1,6)
      EC(4,5)= EC(1,2)
      EC(4,6)=-EC(1,3)
      DO 30 I=2,6
      DO 30 J=1,I-1
      EC(I,J)=-EC(J,I)
   30 CONTINUE
      W1D=W22
      W2D=DDTH(IBAR)
```

```
      IF(INDEX.EQ.3) W1D=0.
      IF(INDEX.EQ.4) W2D=0.
      DO 35 I=1,6
      DO 35 J=1,6
      IF(INDEX.EQ.5) EKG(I,J)=0.0
      EK(I,J)=EK(I,J)-W1D*EM(I,J)+EC(I,J)*W2D+EKG(I,J)
      EC(I,J)=EC(I,J)*W2
      IF(INDEX.EQ.2) EC(I,J)=0.
   35 CONTINUE
   40 CONTINUE
      CALL MAT1(6,A,R,EM,1)
      CALL MAT1(6,EM,A,R,0)
      CALL MAT1(6,A,R,EK,1)
      CALL MAT1(6,EK,A,R,0)
      CALL MAT1(6,A,R,EC,1)
      CALL MAT1(6,EC,A,R,0)
      RETURN
      END

      SUBROUTINE RBK(DDU0)

      IMPLICIT REAL*8(A-H,0-Z)
      COMMON /MKQ1/NGN,NE,NBC(2),NEI(3),N12(10,2),NDOF(2,3)
      COMMON /MKQ2/RL(4),RH0A(3),TH(3),DTH(3),DDTH(3),EA(3),EI(3),
     1 ALX(20),FR(20),TR,DELT
      DIMENSION DDU0(50)
      DO 1 I=1,NGN+2
    1 DDU0(I)=0.
      W12=DTH(1)*DTH(1)
      S1=DSIN(TH(1))
      C1=DCOS(TH(1))
      PN11=RL(1)*C1
      PN12=RL(1)*S1
      VN11=-RL(1)*DTH(1)*S1
      VN12= RL(1)*DTH(1)*C1
      AN11=-RL(1)*(W12*C1+DDTH(1)*S1)
      AN12=-RL(1)*(W12*S1-DDTH(1)*C1)
      DD=RL(4)-PN11
      ALP=DD
```

```
      DD=DD*DD+PN12*PN12
      PHI=DSIGN(90.*TR,ALP)
      IF(DABS(ALP).GT.1.D-20) PHI=DATAN2(-PN12,ALP)
      COSA=0.5*(RL(2)*RL(2)+DD-RL(3)*RL(3))/RL(2)/DSQRT(DD)
      SINA=DSQRT(1.-COSA*COSA)
      ALP=DSIGN(90.*TR,SINA)
      IF(DABS(COSA).GT.1.D-20) ALP=DATAN2(SINA,COSA)
      TH(2)=PHI+ALP
      S2=SIN(TH(2))
      C2=COS(TH(2))
      PN21=PN11+RL(2)*C2
      PN22=PN12+RL(2)*S2
      ALP=PN21-RL(4)
      TH(3)=DSIGN(90.*TR,PN22)
      IF(DABS(ALP).GT.1.D-20) TH(3)=DATAN2(PN22,ALP)
      S3=DSIN(TH(3))
      C3=DCOS(TH(3))
      D=RL(2)*RL(3)*(S2*C3-C2*S3)
      DTH(2)= RL(3)*(VN11*C3+VN12*S3)/D
      DTH(3)= RL(2)*(VN12*S2+VN11*C2)/D
      W22=DTH(2)*DTH(2)
      W32=DTH(3)*DTH(3)
      B1=-AN11+RL(2)*W22*C2-RL(3)*W32*C3
      B2=-AN12+RL(2)*W22*S2-RL(3)*W32*S3
      DDTH(2)=-RL(3)*(B1*C3+B2*S3)/D
      DDTH(3)=-RL(2)*(B2*S2+B1*C2)/D
      NESUM=0
      X=0.0
      I1=NEI(1)
      DO 50 K=1,I1
      NESUM=NESUM+1
      I2=N12(NESUM,2)*3
      X=X+RL(1)/FLOAT(I1)
      DDUO(I2-2)=-X*(W12*C1+DDTH(1)*S1)
      DDUO(I2-1)=-X*(W12*S1-DDTH(1)*C1)
      ALX(NESUM+1) =DDUO(I2-2)*C1+DDUO(I2-1)*S1
   50 DDUO(I2  )=DDTH(1)
      ALX(NEI(1)+1)=DDUO(I2-2)*C2+DDUO(I2-1)*S2
      X=0.0
```

```
      I1=NEI(2)
      IF(I1.EQ.1) GOTO 55
      DO 60 K=1,I1-1
   55 NESUM=NESUM+1
      I2=N12(NESUM,2)*3
      X=X+RL(2)/FLOAT(I1)
      DDUO(I2-2)=AN11-X*(W22*C2+DDTH(2)*S2)
      DDUO(I2-1)=AN12-X*(W22*S2-DDTH(2)*C2)
      DDUO(I2  )=DDTH(2)
      IF(I1.NE.1) ALX(NESUM+1)=DDUO(I2-2)*C2+DDUO(I2-1)*S2
   60 CONTINUE
      I1=NEI(3)
      NESUM=NEI(1)+NEI(2)
      DO 70 K=I1,1,-1
      NESUM=NESUM+1
      I2=N12(NESUM,2)*3
      X=RL(3)-RL(3)/FLOAT(I1)*FLOAT(I1-K)
      DDUO(I2-2)=-X*(W32*C3+DDTH(3)*S3)
      DDUO(I2-1)=-X*(W32*S3-DDTH(3)*C3)
      IF(I1.NE.1.AND.K.NE.I1) ALX(NESUM-1)=DDUO(I2-2)*C3+DDUO(I2-1)*S3
   70 DDUO(I2  )=DDTH(3)
      DDUO(3*N12(1,1))=DDTH(1)
      DDUO(3*N12(NE,1))=DDTH(3)
      DDUO(NGN+1)=DDTH(2)
      DDUO(NGN+2)=DDTH(2)
      ALX(1)=0.
      ALX(NE)=0.
      RETURN
      END

      SUBROUTINE REF

      IMPLICIT REAL*8(A-H,O-Z)
      COMMON /MKQ1/NGN,NE,NBC(2),NEI(3),N12(10,2),NDOF(2,3)
      COMMON /MKQ2/RL(4),RHOA(3),TH(3),DTH(3),DDTH(3),EA(3),EI(3),
     1 ALX(20),FR(20),TR,DELT
      XM1=RHOA(1)*RL(1)
      XM2=RHOA(2)*RL(2)
      XM3=RHOA(3)*RL(3)
```

```
      XJ1=XM1*RL(1)*RL(1)/12.
      XJ2=XM2*RL(2)*RL(2)/12.
      XJ3=XM3*RL(3)*RL(3)/12.
      S1=DSIN(TH(1))
      C1=DCOS(TH(1))
      S2=DSIN(TH(2))
      C2=DCOS(TH(2))
      S3=DSIN(TH(3))
      C3=DCOS(TH(3))
      W12=DTH(1)*DTH(1)
      W22=DTH(2)*DTH(2)
      W32=DTH(3)*DTH(3)
      DDXC1=-0.5*RL(1)*(DDTH(1)*S1+W12*C1)
      DDYC1= 0.5*RL(1)*(DDTH(1)*C1-W12*S1)
      DDXC2=2.*DDXC1-0.5*RL(2)*(DDTH(2)*S2+W22*C2)
      DDYC2=2.*DDYC1+0.5*RL(2)*(DDTH(2)*C2-W22*S2)
      DDXC3=-0.5*RL(3)*(DDTH(3)*S3+W32*C3)
      DDYC3= 0.5*RL(3)*(DDTH(3)*C3-W32*S3)
      FX1=-XM1*DDXC1
      FY1=-XM1*DDYC1
      FX2=-XM2*DDXC2
      FY2=-XM2*DDYC2
      FX3=-XM3*DDXC3
      FY3=-XM3*DDYC3
      FIM1=-XJ1*DDTH(1)
      FIM2=-XJ2*DDTH(2)
      FIM3=-XJ3*DDTH(3)
      A11=-RL(1)*S1
      A12= RL(1)*C1-RL(4)
      A21= RL(2)*S2
      A22=-RL(2)*C2
      B1=-(RL(1)*C1+0.5*RL(2)*C2-RL(4))*FY2+(RL(1)*S1+0.5*RL(2)*S2)*FX2
     1   -0.5*RL(3)*(C3*FY3-S3*FX3)-FIM2-FIM3
      B2= 0.5*RL(2)*(C2*FY2-S2*FX2)-FIM2
      DD=A11*A22-A21*A12
      X1=(B1*A22-B2*A12)/DD
      Y1=(B2*A11-B1*A21)/DD
      X2=-X1-FX2
      Y2=-Y1-FY2
```

```
      I1=NEI(1)
      I2=I1+NEI(2)
      I3=I2+1
      FR(I1)=-X1*C1-Y1*S1
      FR(I2)= X2*C2+Y2*S2
      FR(I3)=-X2*C3-Y2*S3
      DO 100 I=1,3
      IF(NEI(I).EQ.1) GOTO 100
      EL=RL(I)/FLOAT(NEI(I))
      RHOAEL=RHOA(I)*EL
      W22=DTH(I)*DTH(I)
      GOTO (10,20,30), I
   10 IE=NEI(1)
      ID=-1
      GOTO 40
   20 IE=NEI(1)+NEI(2)
      ID=-1
      GOTO 40
   30 IE=NEI(1)+NEI(2)+1
      ID=1
   40 K=0
      I1=IE
   50 I1=I1+ID
      K=K+1
      FR(I1)=FR(I1-ID)-RHOAEL*(ALX(I1-ID)-0.5*EL*W22)
      IF(K.LT.NEI(I)-1) GOTO 50
  100 CONTINUE
      RETURN
      END

      SUBROUTINE MAT(N,A,B,C,IND)

      IMPLICIT REAL*8(A-H,O-Z)
      DIMENSION A(50),B(50,50),C(50)
      DO 20 I=1,N
      A(I)=0.0
      DO 10 J=1,N
      IF(IND.EQ.0) A(I)=A(I)+B(I,J)*C(J)
   10 IF(IND.EQ.1) A(I)=A(I)+B(J,I)*C(J)
```

```
20 CONTINUE
   RETURN
   END

   SUBROUTINE MAT1(N,A,B,C,IND)

   IMPLICIT REAL*8(A-H,O-Z)
   DIMENSION A(6,6),B(6,6),C(6,6)
   DO 30 I=1,N
   DO 30 J=1,N
   A(I,J)=0.
   DO 30 K=1,N
   IF(IND-1) 10,20,20
10 A(I,J)=A(I,J)+B(I,K)*C(K,J)
   GOTO 30
20 A(I,J)=A(I,J)+B(K,I)*C(K,J)
30 CONTINUE
   RETURN
   END
```